TUDelft

Technische Universiteit Delft
Faculteit Elektrotechniek, Wiskunde en Informatica
Delft Institute of Applied Mathematics

Diffusion in a polymeric environment

Verslag ten behoeve van het
Delft Institute of Applied Mathematics
als onderdeel ter verkrijging

van de graad van

BACHELOR OF SCIENCE
in
TECHNISCHE WISKUNDE & TECHNISCHE NATUURKUNDE

door

Paul Donkers

Delft, Nederland
Juni 2017

TUDelft

BSc verslag TECHNISCHE WISKUNDE & TECHNISCHE NATUURKUNDE

"Diffusion in a polymeric environment"

Paul Donkers

Technische Universiteit Delft

Begeleiders

Dr.J.L.A. Dubbeldam
Prof Dr. A. M. Dogterom

Overige commissieleden

Prof. Dr. F.H.J. Redig   Dr. T. Idema

Juni, 2017   Delft

Abstract

Cells of the most common organisms like plants and animals are filled with polymeric networks that fulfil important functions of the cell. There is however no analytically solvable model that describes diffusion in such a cell. This thesis presents a model for diffusion in polymeric environments, and some predictions about the behaviour of the model are made and confirmed by simulations. Furthermore, the Fokker-Planck equation of this problem is studied, in order to solve the problem. Certain approximations are presented and solved, and it is investigated when the approximations are sound. Moreover, a method is described that can derive a solution to an equation with certain boundary conditions, from a solution to the same equation with different boundary conditions. This thesis also shows how this novel method can be applied to this model to find a non-approximated solution to the equation, where this was not possible without this method. Finally, it is described how a multitude of partial differential equations that are linked to each other via the boundary conditions can be solved, can be solved using the method described.

Contents

Chapter 1

Introduction

F-actin networks are found throughout animal, plant and fungal cells. These polymer networks support vital processes, such as muscle contraction, structural strength, cell division and protein transport. These entangled polymers form complex protein networks throughout the cells and influence the diffusion properties of the cell cytoplasm. Since substances necessary for the function of cells, like oxygen, glucose and proteins, transport mostly through diffusion, it is worth knowing about the diffusion properties of an environment consisting of a viscous fluid such as cytoplasm and polymeric networks like F-actin.

An accurate and simple model for the diffusion of a particle in such a network is, however, hard to find. Polymers are per definition highly complex objects and therefore create a high-dimensional problem. The main way in which particles and the polymers influence each other is by short-scale repulsion, a phenomenon hard to describe in a simple manner. It is for example not possible to approximate a repulsion potential with a finite polynomial. Finally, thermal noise drives the motion of polymers and the diffusing particles, meaning that the process becomes highly stochastic.

Several models have been created to describe diffusion in polymeric environments, however, no model has yet proven to be accurate and to be solvable by analytical means[4][6]. In this thesis, a model is developed, and the physical implications of the model are explored as well as the question of whether the model can accurately describe the process. Furthermore, attempts at solving the model are presented. During these attempts, methods are obtained that can be applied to a broader range of cases than just this process.

In the model, a particle diffuses along one axis. Polymers are distributed along this axis at regular intervals. In this way, a string of compartments is created, within which diffusion takes place. Particles can also transfer to a new compartment. This means that there is not one potential for the entire string of compartments, and so individual potentials were considered for each compartment. The Langevin equation to this problem is then used to make predictions about the diffusion rates in several regimes, which are later tested using simulations of this Langevin equation.

Moreover, the Fokker-Planck equation describing this process was derived and several approximations to this equation are studied, as the equation does not prove easily solvable.

Since each compartment satisfies its own potential, we find one Fokker-Planck equation per compartment. These Fokker-Planck equations are of course connected, since the particles can hop change compartments. This connection is trough the boundary conditions for each equation. A method is developed to make sure that such boundary conditions are met. This method inspired a similar but more general method that can solve problems that are solved with other boundary conditions, but that cannot be solved with the boundary conditions of interest. In this way, an exact solution can be acquired.

Chapter 2

Description of situation and model

Throughout this thesis, we will describe the diffusion of a particle in a viscous fluid, that contains a polymeric network. We will assume that the particle itself is a monomer, allowing us to solely regard the translatory motion of the particle, and not concern ourselves with internal motion. While diffusion takes place in three dimensions, we will study the problem in one dimension for simplicity. We consider a periodic structure, with polymer strands perpendicular to the direction along which diffusion can take place, separated by distances of $2\bar{L}$. The behaviour of the particle is only influenced by the two closest polymer strands. The dynamics of the polymer chains which separate the compartments are governed by the Rouse model, with an additional coupling term that describes the influence of the particle on the polymers.

In the Rouse model, the polymer is divided into a number of beads which are considered to be connected by springs. The beads will then move in certain fundamental modes, which satisfy a simple harmonic potential. For each polymer strand, $N/2$ Rouse modes are considered, which gives us N relevant modes per compartment. The centre of mass modes of the polymers are not taken into account, since the polymers are fixed in the network at certain positions, inhibiting significant centre of mass motion. Furthermore, we assume that the viscosity of the fluid is high, so the particle and the polymer cannot accelerate significantly, and speed will be lost quickly. This is called the overdamped limit

2.1   Model equations

We will first describe the dynamics of the particle within a compartment, neglecting the fact that other compartments are present. In the Rouse model, the polymer is described by the amplitude of several fundamental modes, and the centre of mass mode. We will neglect the centre of mass mode, since we do
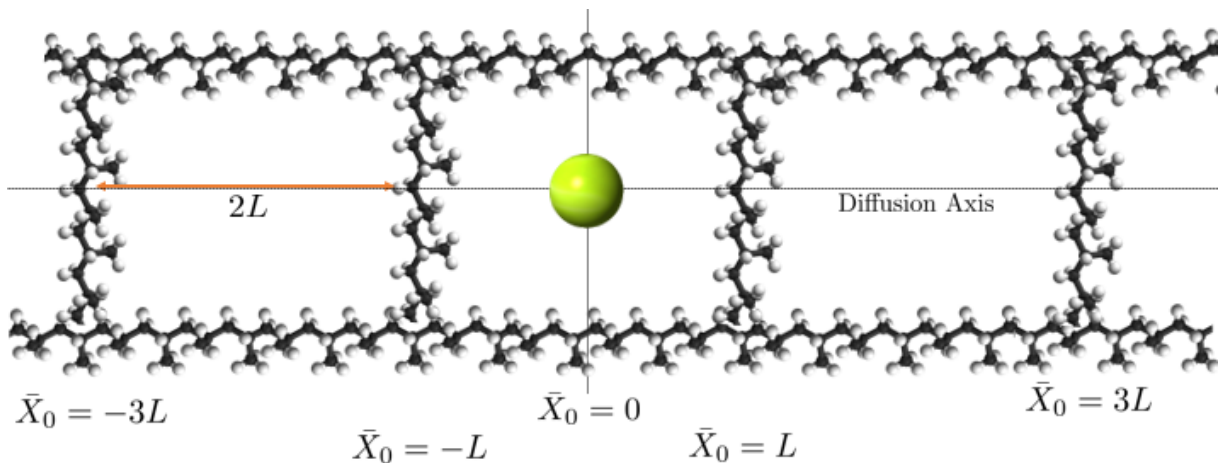
Figure 2.1: A sample of the network with the particle in green
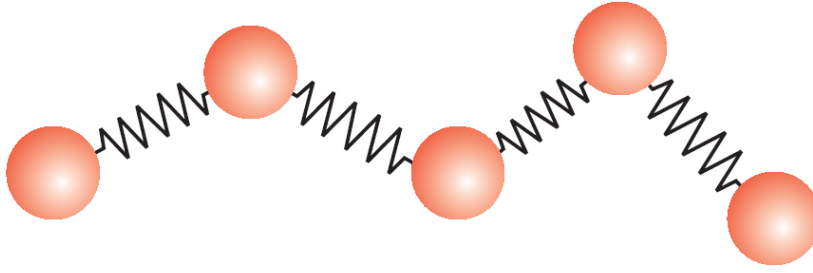
Figure 2.2: A small Rouse chain [5]

not expect the polymer to move about in the fluid, since it is tied at several points in a network. The Rouse model prescribes that the monomer beads, with positions $x = (x_0, \ldots, x_N)^T$ satisfy a potential described by

$$U_h(x) = x^T \kappa x$$

κ accounts for the potential energy stored in the springs. For the matrix κ, only the values $\kappa_{ij} + \kappa_{ji}$ matter, so κ can be chosen symmetric. This means that it can be orthogonally diagonalised as $\kappa = O^{-1} \bar{K} O$. The Rouse modes $\bar{X} = (\bar{X}_0, \ldots, \bar{X}_N)^T$ are subsequently defined as $\bar{X} = Ox$. This means that the modes satisfy a harmonic potential and are not coupled with each other. The first value along the diagonal is zero and corresponds with the centre of mass mode. We will neglect this mode in further study as described above. Looking at the particle position, we see that the particle is most likely trapped between two polymer strands, and will have to cross a certain potential barrier when crossing a strand. The simplest way to express such a potential is a harmonic potential. In this way, the particle potential is similar to the mode potential, which will be expressed by writing $\bar{X}_0$ for the particle position The modes and the particle thus satisfy a harmonic potential

$$U_h(\bar{X}) = \frac{1}{2} \sum_{0=1}^{N} \bar{K}_p \bar{X}_p{}^2$$

For $p \geq 1$, $\bar{X}_p$ is the amplitude of mode p, and $\bar{K}_p$ is the strength of the harmonic potential, and can be read from the diagonal of OKO^{-1}. For $p = 0$, $\bar{K}_0$ is a measure of the strength of the harmonic potential. It is important to be aware of the fact that $\bar{X}_0$ does not refer to the centre of mass mode as is commonly the case.

We also expect some interaction between the beads of the polymer and the particle position. It is hard to derive a specific form, so we assume the simplest form possible for the coupling potential:

$$U_c(x) = (S^T x) \bar{X}_0$$

Here $S = (S_0, S_1, \ldots, S_N)^T$, where each S_i indicates how strong and with what sign a bead couples with the particle. Substituting $x = O^{-1} X$, we can express this coupling potential in terms of the mode displacements to find

$$U_c(\{\bar{X}_p\}) = \Big(\sum_{p=1}^{N} \bar{s_p} \bar{X}_p \Big) \bar{X}_0 \tag{2.1}$$

Here $U_c + U_h$ is the total potential of this system.

The equations of motion are then given by

$$m_p \frac{d^2 x_p}{d\bar{t}^2} = -\bar{\gamma} \frac{dx_p}{d\bar{t}} - \frac{\partial U(x)}{\partial x_p} + \bar{\xi}_p(\bar{t}) = 0$$

Here $p = 0 \ldots N$, m_p is mass of the bead with position x_p, and $\bar{\gamma}$ is the viscosity acting on each bead. Furthermore, $\bar{\xi}$ is thermal noise. A similar equation arises for $\bar{X}_0$. We have already mentioned that we consider the overdamped limit, which means that the inertia is neglected to the viscosity. This gives:

$$\bar{\gamma} \frac{dx_p}{d\bar{t}} = -\frac{\partial U(x)}{\partial x_p} + \bar{\xi}_p(\bar{t})$$

Writing this in matrix form, we see

$$\bar{\gamma}\frac{dx}{d\bar{t}} = -\kappa x + S\bar{X}_0 + \bar{\xi}$$

Here $\bar{\xi} = (\bar{\xi}_0, \ldots, \bar{\xi}_N)$. Substituting $x = O^{-1}X$, we get

$$\bar{\gamma}\frac{d\bar{X}}{d\bar{t}} = -O\kappa O^{-1}\bar{X} + OS\bar{X}_0 + O\bar{\xi}$$

We will now remove the centre of mass mode from the equation and include the particle position $\bar{X}_0$. To do this, we note that in the overdamped limit

$$\bar{\gamma}_0\frac{d\bar{X}_0}{d\bar{t}} = -\bar{K}_0\bar{X}_0 - SO^{-1}\bar{X} + \bar{\Xi}_0(t)$$

Here $\bar{\gamma}_0$ is the particle's viscosity, and $\bar{\xi}_0(t)$ is thermal noise acting on the particle. We find that the total equation becomes

$$\bar{\Gamma}^T\frac{d\bar{X}}{d\bar{t}} = -\bar{\Theta}\bar{X} + \bar{\Xi}$$

Here $\bar{\Gamma} = (\bar{\gamma}_0, \bar{\gamma}, \ldots, \bar{\gamma})^T$, $\bar{\Xi} = (\bar{\Xi}_0, (O\bar{\xi})_1, \ldots, (O\bar{\xi})_N)$ and

$$\bar{\Theta} = \begin{pmatrix} \bar{K}_0 & \bar{s}_1 & \cdots & \bar{s}_N \\ \bar{s}_1 & \bar{K}_1 & \cdots & 0 \\ \vdots & \vdots & \ddots & \vdots \\ \bar{s}_N & 0 & \cdots & \bar{K}_N \end{pmatrix}$$

Here $(\bar{s}_1, \ldots, \bar{s}_N) = SO = (O^{-1}S^T)^T$. The last equality follows from the fact that Θ was orthogonally diagonalised, and thus $O^T = O^{-1}$.

In these equations $\bar{\xi}_p(\bar{t})$ is Gaussian white noise, where $\langle\bar{\xi}_p(\bar{t})\rangle = 0$. For $\langle\bar{\xi}_p(\bar{t})\bar{\xi}_q(\bar{s})\rangle$, we resort to the fluctuation-dissipation theorem. This theorem is a fundamental relation in statistical physics which says that fluctuation and dissipation of energy are governed by the same physical process. In this process thermal noise is the fluctuation, and the viscosity is the cause of dissipation of energy. This theorem also quantitatively relates fluctuation and dissipation, which gives, and by the fluctuation-dissipation theorem $\langle\bar{\xi}_p(\bar{t})\bar{\xi}_q(\bar{s})\rangle = 2\bar{\Gamma}_p k_B T\delta_{pq}\delta(t-s)$. Due to the orthogonal nature of O, this also means $\langle\bar{\Xi}_p(\bar{t})\bar{\Xi}_q(\bar{s})\rangle = 2\bar{\Gamma}_p k_B T\delta_{pq}\delta(t-s)$.

Physically we can interpret these results by saying that the system satisfies a potential

$$U = \frac{1}{2}\sum_{p=0}^{N}\bar{K}_p\bar{X}_0^2 + (\sum_{p=0}^{N}\bar{s}_p\bar{X}_p)\bar{X}_0$$

The equations of motion are then given by

$$\bar{\gamma}_p\frac{d\bar{X}_p}{d\bar{t}} = -\frac{\partial U}{\partial\bar{X}_p} + \bar{\Xi}_p(t)$$

Here $\gamma_p = \gamma_0$ the damping constant of the particle for $p = 0$, and $\gamma_p = \gamma$ the damping constant of the beads for $p \geq 1$. An important consequence of this derivation is that γ_p is the same for $p \geq 1$

Once $|\bar{X}_0| > \bar{L}$, the particles moves into the next compartment, where it satisfies the same equations, but shifted by $2\bar{L}$

2.2   Dimensionless equation

We will now proceed to derive a dimensionless representation of these equations, in order to obtain a clearer image of relevant quantities. To do this, we define the dimensionless quantities $X_p = \bar{X}_p\sqrt{\frac{\bar{K}_0}{k_BT}}$, $t = \bar{t}\frac{\bar{K}_0}{\bar{\gamma}_0}$, $s_p = \frac{\bar{s}_p}{\bar{K}_0}$, $\gamma_p = \frac{\bar{\gamma}_p}{\bar{\gamma}_0}$, $K_p = \frac{\bar{K}_p}{\gamma_p\bar{K}_0}$ and $\xi_p(t) = \frac{\bar{\xi}_p(t)}{\gamma_p\sqrt{\bar{K}_0 k_BT}}$.

We then see that

$$\frac{dX}{dt} = -\Theta X + \Xi \tag{2.2}$$

Here $X = (X_0, X_1, \ldots, X_N)^T$ and $\Xi = (\xi_0, \xi_1, \ldots, \xi_N)^T$. Furthermore

$$\Theta = \begin{pmatrix} 1 & s_1 & \cdots & s_N \\ \frac{s_1}{\gamma_1} & K_1 & \cdots & 0 \\ \vdots & \vdots & \ddots & \vdots \\ \frac{s_N}{\gamma_N} & 0 & \cdots & K_N \end{pmatrix} \tag{2.3}$$

Note that like $\bar{\xi}_p$, ξ_p is Gaussian white noise with $\langle \xi_p(t) \rangle = 0$, but now with amplitude $\langle \xi_p(t)\xi_q(s) \rangle = \frac{2}{\gamma_p}\delta_{pq}\delta(t-s)$. The dimensionless compartment length is given $L = \bar{L}\sqrt{\frac{\bar{X}_0}{k_b T}}$. Processes with the form of equation 2.3 are called multidimensional Ornstein-Uhlenbeck processes. Throughout this thesis, the methods used are sought to be valid for general cases of the Ornstein-Uhlenbeck processes, thus for general Θ and Ξ whenever possible. Equation 2.2 is the Langevin equation of this process. It describes single outcomes of a stochastic process, as functions of a noise function

Chapter 3

Predictions

Before attempting to solve this problem, we can make some judicious guesses about the expected behaviour of the particle. Diffusion-like processes are commonly described as:

$$\sigma^2 = Dt^\alpha \tag{3.1}$$

Here σ^2 is the variance of the particle position. For regular diffusion, we find $\alpha = 1$, which means that $\frac{d(\sigma^2)}{dt}$ is constant. This implies that the diffusion behaviour does not change with increasing time or variance. We also identify the cases where $\alpha < 1$, called sub-diffusion, and $\alpha > 1$, which is super-diffusion. In these two cases, the rate of diffusion either decreases or increases with time. The three different cases can be seen in figure 3.1. When a particle moves with a constant speed, we find ballistic motion, with
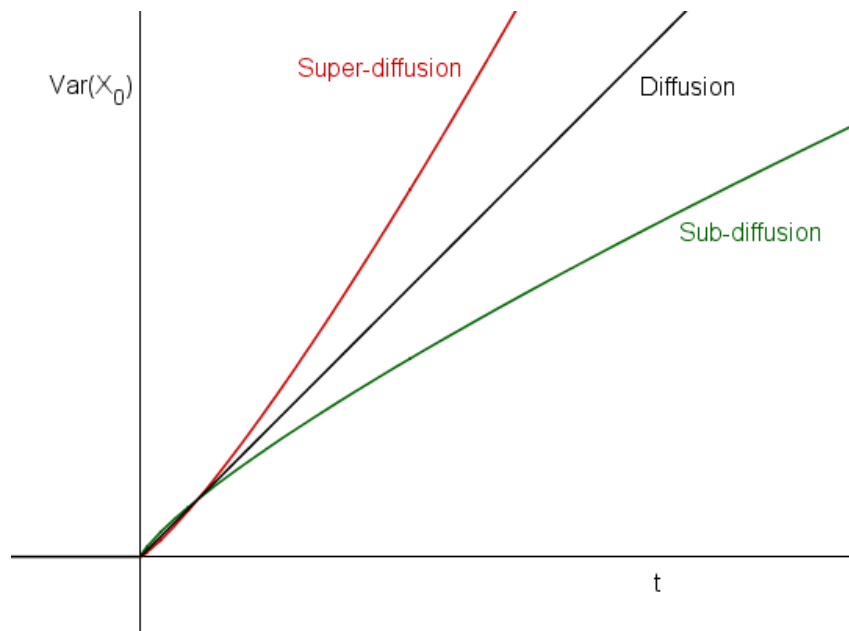
Figure 3.1: Variance of particle position for $\alpha = 1.2$ (super-diffusion), $\alpha = 1$ (regular-diffusion) and $\alpha = 0.8$ (sub-diffusion)

$\alpha = 2$. Most super-diffusive processes are limited at $\alpha = 2$ since the thermal noise inhibits the particle from moving in one direction only. Experimental studies concerning F-actin find sub-diffusion for certain cases [2], so we might expect some anomalous diffusion, or $\alpha \neq 1$ to take place. The most interesting cases are for $\alpha \neq 1$, and otherwise D can be studied.

While making predictions about D and foremost α, we will identify several regimes.

3.1 Large times

For timescales for which most particles have switched compartments a considerable amount of times, the average squared displacement is mostly determined by the compartment in which a particle resides, rather than the specific position within that compartment. If we only consider the compartment the particle is in, we have a process that resembles a one-dimensional random walk, where at every time step, the particle has the options to move either one unit of length to the right, or to the left. There are however two important differences between this process and a simple random walk

One difference is that once a particle has entered a compartment, it does not have an equal chance of leaving the compartment through either the left or the right-hand side of the compartment. When a particle enters a compartment from the left-hand side, it initially is in the left-hand side of the compartment, and we might thus expect the particle to have a larger chance of quickly exiting the compartment on the left-hand side, than quickly leaving through the right-hand side. If a particle has entered the compartment from the right-hand side, it is, of course, more likely to leave the compartment through this side than through the left-hand side. Once a particle has reached the centre of the compartment, this bias is mostly gone and is only preserved by the mode amplitudes. This implies that if the harmonic potential is so strong that most particles cross the centre of the compartment before leaving the compartment, this bias can be neglected. If this tendency of moving towards the previous compartment is significant we obviously expect the diffusion to be slower. Looking at equation 3.1 the question arises of whether this slow diffusion expresses itself in a low D, or in a low α. For a regular random walk, we find regular diffusion and thus $\alpha = 1$, which implies that $\frac{d\sigma^2}{dt}$ is constant and that the diffusion process does not change with time or variance of the process. Looking at our bias, we have no reason to expect that the bias would be more or less significant for larger t or σ^2, as long as the average squared displacement is large. We, therefore, predict the α to remain 1 under this alteration of Brownian motion, and thus we expect D to be lower than for regular diffusion, due to this bias.

The second difference with a simple random walk is that the time between a change in compartments is not a constant, but is a stochastic process itself. Like in the previous section, we do not expect this difference to specifically change diffusion speed for larger or smaller times or variances, and thus we do not expect this process to have an effect on α. Whether this stochastic waiting time would make D larger or smaller, entirely depends on how the typical waiting times for the stochastic process compare to the constant waiting time. It is, for instance, clear that if for a simple random walk the constant waiting time is far larger than the waiting time the stochastic process is expected to yield, the simple random walk will diffuse much slower than for this random walk with stochastic waiting time.

We can conclude that for large times we find something similar to a random walk, and thus expect $\alpha = 1$, implying regular diffusion. There are some ways in which this process differs from a random walk, but these differences are not expected to alter α and cause sub- or super-diffusion

3.2 Short times, small coupling

We will now look at shorter timescales, in which most particles have not left the initial compartment. We will find that we have entirely different behaviour for large and small coupling, and we will thus consider them separately.

For small coupling, the diffusion process is governed by the harmonic potential of the particle. The influence of the Rouse modes can be neglected. If a particle is initially situated in the centre of a compartment, the harmonic force $-X_0$ is small for small times, and the harmonic potential can be neglected for very small times. We then have regular diffusion with $\alpha = 1$. For larger times we expect the variance to reach an equilibrium value, since at a certain point the strong harmonic force $-X_0$ inhibits further diffusion of the particle. This equilibrium can of course only take place if the standard deviation in this equilibrium is significantly lower than the distance to the boundary of the compartment. If this is not the case, many particles will have left the compartment before an equilibrium variance is reached. We, therefore, expect that for large compartments, the diffusion coefficient changes from an initial $\alpha = 1$, to an eventual $\alpha = 0$ belonging to constant variance. If L is not large enough, α will not reach 0, as too many particles have crossed the first polymer strand into a second compartment by then. However, it is reasonable to expect α to lower slightly as time increases.

In conclusion, we expect that for small coupling α will start at 1, then decreases towards 0, and will then for longer time ranges increase to a value of 1 again.

3.3 Short times, large coupling

In this section, the regime where the coupling between the polymer and the particle is significantly stronger than the harmonic potential will be described. We will entirely neglect the harmonic potential in this analysis. Without loss of generality, we will assume all coupling constants to be positive. Assume that initially, the particle moves to the right slightly. All modes will be pushed towards negative values, since the coupling force $-\frac{s_p}{\gamma_p}X_0$ is negative. This causes $-\sum_{p=1}^{N}s_pX_p$ to become positive, thus pushing the particle to the right. This on its turn violently pushes all the modes towards negative values. This process repeats itself, constantly pushing the particle to the right, and the modes towards negative values. The particle will thus be catapulted to the first polymer strand.

Since the forces scale with the displacement, the strength of this process increases. The particle will enjoy super-diffusion, or an α larger than 1. We expect α to increase over time, as the strength of the process increases with the increasing displacement. There is no reason for α to converge to any specific value, so we could predict α to unlimitedly increase from an initial value of 1 until the standard deviation is such that particle will enter new compartments. Solving the equation for no noise gives an exponentially increasing particle position.

In the most cases of super-diffusion, α is limited at 2, since this describes the ballistic motion of an unhindered particle. In processes that bear resemblance to diffusion, the particle is in some way hindered, causing α to be lower than 2. In this case, however, the particle is not hindered at all. On the contrary, its motion is only amplified due to coupling, which is the reason why this particle might "diffuse" super-ballistically.

It is important to note that α will not increase indefinitely since at one point the compartment boundaries are reached, so we might not observe the super-ballistic motion.

We can extend our time scale slightly, to also allow a particle to have crossed a polymer strand once. We then find something remarkable. We have seen that particles are pushed towards a polymer strand rather quickly. Once they reach this strand, they reach the next compartment. If a particle has crossed a boundary from left to right, it has a negative value of X_0 in the new compartment. The coupling process then causes this value of X_0 to rapidly become even more negative, until the same boundary is crossed again. The particle is then through coupling again quickly pushed back to the polymer strand. The particle is in this way confined to a polymer strand.

As a result, strong coupling causes the particle to quickly move from the centre of a compartment to a polymer strand, where they are trapped by the coupling process. Subsequently, the particle might diffuse from polymer strand to polymer strand, rather than from compartment to compartment. In this way, strong coupling causes a process alike a process with large harmonic potential, with the difference that the positions at which particles are trapped are at the polymer strands, instead of right in between two polymer strands. This would imply the variance to quickly move to L^2 from where regular diffusion will take place.

Looking at α, we see that the process will start with free diffusion, and an α of 1. α will then increase until a significant amount of particles are trapped at a polymer strand. When this happens, the variance will reach a plateau and α will become 0. On even longer timescales, the particle will diffuse like a random walk, and α will be 1.

This behaviour of residing at the polymer strands is not what we would physically expect. It is, therefore, a reason to suspect that the model might be flawed. This does not have to be the case, as the regime where the coupling is much stronger than the harmonic potential, clearly is not a relevant regime. Still, this section is a reason to become weary of the model

Chapter 4

Fokker-Planck equation

The Langevin description used above is an intuitive description of the process and is therefore easy to formulate. This is the reason why we started by determining a Langevin description. One important feature of this process is, however, not incorporated in this description. That feature is what happens when the particle reaches the points $X_0 = L$ and $X_0 = -L$. At these points, the particle crosses a polymer strand and moves into a neighbouring compartment. It is then governed by the same system of equations shifted in the X_0 dimension by $2L$, since the centre of the compartment now is at $2L$ instead of at 0. This means that we in fact have

$$\frac{dX}{dt} = -\Theta \sum_{i=-\infty}^{\infty} H(X_0 - 2iL)(X - (2iL, 0, \dots)^T) + \Xi$$

Here H is a block function with $H(x) = 1$ for $-L < x \leq L$ and $H(x) = 0$ for all other x. The dynamics are governed by equation 2.2, where X_0 is centred around the centre of the compartment the particle is in. It is unclear what happens with the mode displacements when a new compartment is entered, so it is chosen to reset those displacements to zero. This makes the process even more complex. Such a periodic and at certain points non-continuous description can be incorporated in the Langevin description, but due to the non-continuous nature of the equation, we do not expect an analytical result can be obtained. Note that the result will of course be continuous, but that the forces acting on the particle are not continuous with the particle position. Therefore, we resort to the Fokker-Planck equation of this process.

The Langevin equation of a process describes specific realisations, whose outcomes are stochastic due to the stochastic nature of the thermal noise. The Fokker-Planck describes the probability density function of the particle position and the mode displacements, in a partial differential equation. This equation has a t dimension with boundaries at 0 and infinity, N $(X_p)_{p \geq 1}$ dimensions with boundaries at minus and plus infinity and an X_0 dimension with boundaries at $-L$ and L. The initial condition forms a boundary condition at $t = 0$, and for the $p \geq 1$ modes, the boundary conditions are physical boundary conditions, which imply that the probability density is 0 at plus and minus infinity. The boundaries for X_0 are more interesting. These boundaries are the reason for choosing the Fokker-Planck equation.

We will first look at an isolated compartment. We assume that the particle can move out of the compartment, but can never enter the compartment again. Once the particle has reached a polymer strand, it is removed from the system. The probability of residing at the boundaries is therefore zero. We thus impose homogeneous Dirichlet boundary conditions of zero amplitude at the boundaries. This boundary condition is referred to as absorbing.

Later in this thesis, we will study multiple adjacent compartments and the boundary conditions needed to connect these compartments. These conditions are the continuity of probability flux and the continuity of probability at the boundary. Eventually we will consider a set of partial differential equations, each describing a different compartment. We will study this in more detail in later sections.

4.1   Fokker-Planck equation

We can deduce the Fokker-Planck equation for a compartment from equation 2.2. The Fokker-Planck equation for this equation is given by [7]:

$$\frac{\partial p(X,t)}{\partial t} = \sum_{p=0}^{N} \left(\frac{\partial}{\partial X_p} \big((\Theta X)_p p(X,t) \big) + \frac{1}{2} \frac{\partial^2}{\partial X_p^2} \Big(\mathbb{E}\big(\Xi_p(t)^2\big) p(X,t) \Big) \right)$$

Here $(\Theta X)_p$ is the p'th value of ΘX. From this equation we directly derive the Fokker-Planck equation we will use throughout this thesis

$$\frac{\partial p(X,t)}{\partial t} = \sum_{p=0}^{N} \left(\Theta_{pp} p(X,t) + \sum_{i=0}^{N} \Theta_{pi} X_i \frac{\partial}{\partial X_p} p(X,t) + \frac{1}{\gamma_p} \frac{\partial^2}{\partial X_p^2} p(X,t) \right) \tag{4.1}$$

4.2   Escape rate

We will use the differential equation for p to determine the chance of a particle leaving the interval $[-L, L]$ on either side of the interval. We will derive an expression for the time derivative of the chance of the particle being in the interval $[-L, L]$.

We will integrate $\frac{\partial p}{\partial t}$ over all modes consecutively using the partial differential equation, to derive the escape rate. For this process, we use mathematical induction on the well-ordered set $\{0, \ldots, N\}$. This procedure can be found in Appendix A. For the marginal probability density $p(X_0, t)$ of $p(X,t)$ in X_0 we find

$$\frac{\partial p(X_0, t)}{\partial t} = \Theta_{00} p(X_0, t) + \Theta_{00} X_0 \frac{\partial p(X_0, t)}{\partial X_0} +$$

$$\frac{\partial^2 p(X_0, t)}{\partial X_0^2} + \frac{\partial}{\partial X_0} \sum_{i=1}^{N} \Theta_{0i} \int X_i p(X,t) d(\{X_j\}_{j \geq 1})$$

Integrating this expression over the interval $[-L, L]$, we find that the escape rate, is given by

$$-\frac{\partial}{\partial t} \int_{-L}^{L} p(X_0, t) dX_0 = -\frac{\partial p(X_0, t)}{\partial X_0}\big|_{-L}^{L} - X_0 p(X_0, t)\big|_{-L}^{L} -$$

$$\sum_{i=1}^{N} \Theta_{0i} \int X_i p(X,t) d(\{X_j\}_{j \geq 1})\big|_{X_0=-L}^{X_0=L}) \tag{4.2}$$

Note that the $X_0 p(X_0, t)_{-L}^{L}$, as well as the integral term, drop out for homogeneous Dirichlet, that is absorbing, boundary conditions. Since we will not assume these boundary conditions when studying multiple compartments, we will not drop those terms from the equation. From equation 4.2, it is easy to distinguish the escape rate through the boundary on the left or right-hand side.

The $\frac{\partial p(X_0,t)}{\partial X_0}$ term is typical of a diffusion process and is reminiscent of Fick's and Fourier's law, which describe diffusion of mass and energy respectively, rather than probability.

The $-X_0 p(X_0, t)$ term implies that the more likely it is for a particle to be positioned at the boundaries, the smaller the escape rate. This might seem contradictory, as we might expect a higher escape rate when the probability is high in a certain compartment. This scaling, however, is represented, as in all diffusion systems, by the place derivative as previously discussed. The term $-X_0 p(X_0, t)$ therefore represents the force that results from the harmonic potential in X_0, that makes the particle tend to the centre of the compartment. This force obviously decreases the probability flux out of the compartment and scales with p at the boundary.

For the $\sum_{i=1}^{N} \Theta_{0i} \int X_i p(X,t) d(\{X_j\}_{j \geq 1})\big|_{X_0=-L}^{X_0=L}$ term, it is important to note that $\int X_i p(X,t) d(\{X_j\}_{j \geq 1}) = \mathbb{E}(X_i|X_0) p(X_0, t)$. This term thus scales with the sum over all modes, of the product of the coupling constant between the mode and particle position, and the expected value of the mode displacement at the boundary. The term is, therefore, a measure of the expected force that all modes exerts on the particle through coupling. This coupling force can push the particle to the centre of the compartment or towards the boundary. In this way, the coupling force influences the probability flux. The term also scales with the marginal probability density at the boundary, since the d coupling force has more impact when the particle has a larger probability of residing at the boundary.

Chapter 5

Approximations to Fokker-Planck equation

We will first consider the partial differential equation in one compartment. The equation then satisfies absorbing boundary conditions. These mean that the probability of finding the particle at the boundary is zero. This physically means that as soon as a particle hits the boundary, it is removed from the system, and will not return to the cell.

A common approach to solving the equation would be to apply separation of variables. This method is not possible in this form of the equation, since mixed terms like $X_i \frac{\partial p}{\partial X_p}$ appear in the equation. A common way to solve this problem is to change the variables into a system that does not contain these coupled terms. This would equal diagonalising Θ. The problem is then that the boundaries of the compartments are not specified by a value of one variable, such as $X_0 = L$, but depend on a number of variables. The bounding planes then are not orthogonal to the axis belonging to some variable, and so after diagonalising the equation, separation of variables is still not applicable.

We will proceed to rewrite the Fokker-Planck equation into a different form and investigate certain possible approximations, which drop the mixed terms. This allows separation of variables. The reason why these approximations are not made in the original equation is because this removes aspects of the process from the equation, while we hope that in this different form, we can drop mixed terms while still conserving the properties of the process.

5.1 Analogous representation

We write $p = \exp(X^T H X)q$ for a certain matrix H, and then study the function q, in order to remove mixed terms. From derivations in Appendix B we find:

$$\frac{\partial q}{\partial t} = \sum_{p=0}^{N} \left(\frac{\partial^2 q}{\partial X_p^2} \frac{1}{\gamma_p} + \frac{\partial q}{\partial X_i} \sum_{j=0}^{N} \left(\frac{2}{\gamma_p} (H_{pj} + H_{jp}) + \Theta_{pj} \right) X_j \right.$$

$$\left. + q(X,t) \left(\left(\sum_{j=0}^{N} (H_{pj} + H_{jp}) X_j \right) \left(\sum_{j=0}^{N} \left(\frac{1}{\gamma_p} (H_{pj} + H_{jp}) + \Theta_{pj} \right) X_j \right) + \frac{2}{\gamma_p} H_{pp} + \Theta_{pp} \right) \right)$$

We now have mixed terms in the forms $\frac{\partial q}{\partial X_i} X_j$ and $X_i X_j$. By choosing H cleverly, we can try to eliminate as much of these two terms. If we want to remove the term with the first derivative, we need $\frac{2}{\gamma_p} (H_{pj} + H_{jp}) + \Theta_{pj} = 0$ for all p and j. This is only possible if $\Theta_{ij}\gamma_i = \Theta_{ji}\gamma_j$. Fortunately this is the case, which is the direct result of the fluctuation-dissipation theorem. The theory derived from this analogous representation is therefore no longer valid for general Θ and Ξ. We choose $H_{pj} = -\frac{\gamma_p}{4}\Theta_{pj}$, and find

$$\frac{\partial q}{\partial t} = \sum_{p=0}^{N} \left(\frac{\partial^2 q}{\partial X_p^2} \frac{1}{\gamma_p} + q(X,t) \left(-\frac{\gamma_p}{4} (\Theta X)_p^2 + \frac{\Theta_{pp}}{2} \right) \right) \tag{5.1}$$

This equation still contains the mixed term $(\Theta X)_p^2$. Certain approximations will be studied that overcome this problem.

21

5.2   Small compartment

For small compartments, the length over which p and therefore q changes, becomes relatively short, while the expected typical amplitude of p and so of q will not be smaller. This could cause $\frac{\partial^2 q}{\partial X_0^2}$ to be far larger than $\frac{\partial^2 q}{\partial X_p^2}$ for $p \geq 1$, and so we could neglect $\frac{\partial^2 q}{\partial X_p^2}$ for $p \geq 1$. We then find

$$\frac{\partial q}{\partial t} = \frac{\partial^2 q}{\partial X_0^2} \frac{1}{\gamma_p} + q(X,t) \sum_{p=0}^{N} \left(- \frac{\gamma_p}{4} (\Theta X)_p^2 + \frac{\Theta_{pp}}{2} \right)$$

Substituting $q = \exp(-\lambda t) Q(X)$, the eigenfunction equation is of the form

$$\frac{\partial^2 Q(X)}{\partial X_0^2} \frac{1}{Q(X)} = c X_0^2 + f(\{X_p\}_{p \geq 1}) Y_0 + g(\{X_0\}_{p \geq 1}) - \lambda$$

Parabolic cylinder functions solve the equation $\frac{\partial^2 f}{\partial x^2} = ax^2 + bx + c - \lambda$ [1] As a result, this eigenfunction equation is solved by parabolic cylinder functions where $\{X_p\}_{p \geq 1}$ act at as parameters and X_0 as the variable, multiplied by a function of $\{X_p\}_{p \geq 1}$. Note that the eigenvalue will therefore generally depend on $\{X_p\}_{p \geq 1}$. Eigenfunctions will thus decay at different rates for different $\{X_p\}_{p \geq 1}$.

5.3   Large compartment

For a large interval, on the contrary, we expect $\frac{\partial^2 p}{\partial X_0^2}$ and so $\frac{\partial^2 q}{\partial X_0^2}$ to be relatively small. We can then neglect this term. Since the equation then does not contain any X_0 derivatives, we can multiply any solution q with an arbitrary function $f(X_0)$ and obtain a different solution. This adjusted equation, therefore, does not predict much about the X_0 behaviour. Since we are mostly concerned about the X_0 dependency, neglecting the second X_0 derivative will not generate fruitful results.

5.4   Small mode displacement

We will now consider the case where the mode displacement of the polymer is relatively small compared to the amplitude of the particle. Note that this cannot hold for an entire domain since the region around $X_0 = 0$ will always be included. Furthermore, large parts of our domain do have large mode amplitudes, but we assume that the probability there is so small, that any mistakes made there are not significant.

The approximation we will make neglects all the $\{X_p\}_{p \geq 1}$ terms in the $(\Theta X)_p$ term. This would be valid for small mode displacement. This approximation gives:

$$\frac{\partial q}{\partial t} = \sum_{p=0}^{N} \left(\frac{\partial^2 q}{\partial X_p^2} \frac{1}{\gamma_p} + q(X,t) \left(- \frac{\gamma_p}{4} \Theta_{p0}^2 X_0^2 + \frac{\Theta_{pp}}{2} \right) \right)$$

We see that mixed terms such as $X_p X_j$ are not present in this equation, which means we can apply separation of variables. Before we continue solving this equation, we transform this new equation back to an altered equation for p, to enable us to check whether the made approximation is sound. We find the equation:

$$\frac{\partial p}{\partial t} = \sum_{p=0}^{N} \left(\frac{1}{\gamma_p} \frac{\partial^2 p(X,t)}{\partial X_p^2} + \sum_{j=0}^{N} \Theta_{pj} X_j \frac{\partial p(X,t)}{\partial X_p} + p(X,t) \left(\Theta_{pp} + \frac{\gamma_p}{4} \left((\sum_{j=0}^{N} \Theta_{pj} X_j)^2 - \Theta_{p0} X_0^2 \right) \right) \right)$$

The approximation thus adds a term $p(X,t) \left(\sum_{p=0}^{N} \frac{\gamma_p}{4} \left((\sum_{j=0}^{N} \Theta_{pj} X_j)^2 - \Theta_{p0} X_0^2 \right) \right)$. This term is small for regions of relatively small displacement, which means that this approximation is sound. It is important to note that we have not ignored coupling, while we have removed the difficulties that coupling causes by introducing mixed terms. Since this not easily achieved in the equation for p, we can see why we would go through the hassle of studying the function q.

We will now solve this altered equation with homogeneous boundary conditions and a source term, from we will deduce the Green's function. We will denote the source term in the p domain as $V(X,t)$. In the q domain, this adds a term $\tilde{V}(X,t) = \exp(-X^T H X)V(X,t)$.

Looking at our approximated equation for q, we see find the eigenfunction equation

$$\sum_{p=0}^{N} \left(\frac{\partial^2 Q(X)}{\partial X_p^2} \frac{1}{\gamma_p} + Q(X)\left(-\frac{\gamma_p}{4}\Theta_{p0}^2 X_0^2 + \frac{\Theta_{pp}}{2} \right) \right) + \lambda Q(X) = 0 \tag{5.2}$$

We will apply separation of variables and substitute $Q(X) = R(X_0)S(\{X_p\}_{p\geq 1})$, which gives

$$\frac{1}{S(\{X_p\}_{p\geq 1})}\sum_{p=1}^{N}\left(\frac{\partial^2 S(\{X_p\}_{p\geq 1})}{\partial X_p^2} \frac{1}{\gamma_p} \right) + \frac{1}{R(X_0)}\frac{\partial^2 R(X_0)}{\partial X_0^2} + \sum_{p=0}^{N}(-\frac{\gamma_p}{4}\Theta_{p0}^2 X_0^2 + \frac{\Theta_{pp}}{2}) + \lambda = 0$$

This gives parabolic cylinder functions for $R(X_0)$ for countably infinite eigenvalues. $S(\{X_p\})$ is solved by $\exp(i\sum_{p=1}^{N}\omega_p X_p)$. This creates an N-fold uncountably infinite set of eigenvalues, and allows standard Fourier analysis.

Let B_n be solution to the equation

$$\frac{\partial^2 B_n(X_0)}{\partial X_0^2} + (-\sum_{p=0}^{N}\frac{\gamma_p}{4}\Theta_{p0}^2 X_0^2 + \mu_n)B_n(X_0) = 0$$

Note that this equation is a regular Sturm-Liouville equation. Thus, the eigenfunctions form a complete set. The solutions for equation 5.2 are then given by

$$B_{n,\{\omega\}}(X) = \exp(i\sum_{p=1}^{N}\omega_p X_p)B_n(X_0)$$

With eigenvalues $\lambda = \sum_{p=1}^{N}\frac{\omega_p^2}{\gamma_p} - \sum_{p=0}^{N}\frac{\Theta_{pp}}{2} + \mu_n$ Since the eigenfunctions B_n and the complex exponentials $\exp(i\sum_{p=1}^{N}\omega_p X_p)$ both form complete sets on their respective domains, we deduct that the eigenfunctions $B_{n,\{\omega\}}$ form a complete set themselves on $[-L,L]\times\mathbb{R}^N$. Hence, we know that the solution to the equation for q can be written as

$$q(X,t) = \sum_{n=1}^{\infty}\int_{\mathbb{R}^N} b_{n,\{\omega\}}(t)B_{n,\{\omega\}}(X)d\{\omega_p\}_{p\geq 1}$$

Since the eigenfunctions as well as q satisfy the same homogeneous boundary conditions, we can differentiate term-by-term with respect to X and t. This gives:

$$\sum_{n=1}^{\infty}\int_{\mathbb{R}^N} \frac{db_{n,\{\omega\}}(t)}{dt}B_{n,\{\omega\}}(X)d\{\omega_p\}_{p\geq 1} =$$

$$-\sum_{n=1}^{\infty}\int_{\mathbb{R}^N} \lambda_{n,\{\omega\}}b_{n,\{\omega\}}(t)B_{n,\{\omega\}}(X)d\{\omega_p\}_{p\geq 1} + \tilde{V}(X,t)$$

We can also express $\tilde{V}$ as a sum of eigenfunctions, in order to derive differential equations for the coefficients $b_{n,\{\omega\}}$.

$$\tilde{V}(X,t) = \sum_{n=1}^{\infty}\int_{\mathbb{R}^N} c_{n,\{\omega\}}(t)B_{n,\{\omega\}}(X)d\{\omega\}_{p\geq 1}$$

Here

$$c_{n,\{\omega\}}(t) = \left(\frac{1}{2\pi}\right)^N \frac{1}{\langle B_n, B_n\rangle}\int_{-L}^{L}\iint_{\mathbb{R}^N}\tilde{V}(X,t)B_n(X_0)\exp(-i\sum_{p=1}^{N}\omega_p X_p)d\{X_p\}_{p\geq 1}dX_0$$

We then get the following equation for $b_{n,\{\omega\}}$:

$$\frac{db_{n,\{\omega\}}}{dt} = -\lambda_{n,\{\omega\}}b_{n,\{\omega\}} + c_{n,\{\omega\}}(t)$$

This is easily solved by

$$b_{n,\{\omega\}} = \exp(-\lambda_{n,\{\omega\}}t)(b_{n,\{\omega\}}(0) + \int_0^t \exp(\lambda_{n,\{\omega\}}\tau)c_{n,\{\omega\}}(\tau)d\tau)$$

Furthermore, $b_{n,\{\omega\}}(0)$ can be computed in a similar way to $c_{n,\{\omega\}}(t)$, giving

$$b_{n,\{\omega\}}(0) = \left(\frac{1}{2\pi}\right)^N \frac{1}{\langle B_n, B_n\rangle} \int_{-L}^L \iint_{\mathbb{R}^N} q(X,0)B_n(X_0)\exp(-i\sum_{p=1}^N \omega_p X_p)d\{X_p\}_{p\geq 1}dX_0$$

Then q is given by

$$q(X,t) = \left(\frac{1}{2\pi}\right)^N \int_{-L}^L \iint_{\mathbb{R}^N} \sum_{n=1}^\infty \frac{B_n(X_0)B_n(\tilde{X}_0)}{\langle B_n, B_n\rangle}$$

$$\left(p(\tilde{X},0)\iint_{\mathbb{R}^N} \exp(i\sum_{p=1}^N \omega_p(X_p - \tilde{X}_p))\exp(-\lambda_{n,\{\omega\}}t)d\{\omega\}\right.$$

$$\left.+\int_0^t \tilde{V}(\tilde{X},\tau)\iint_{\mathbb{R}^N}\exp(i\sum_{p=1}^N \omega_p(X_p - \tilde{X}_p))\exp(-\lambda_{n,\{\omega\}}(t-\tau))d\{\omega\}d\tau\right)d\{\tilde{X}_p\}_{p\geq 1}d\tilde{X}_0$$

We see

$$\iint_{\mathbb{R}^N}\exp(i\sum_{p=1}^N \omega_p(X_p - \tilde{X}_p))\exp(-\lambda_{n,\{\omega\}}t)d\{\omega\} =$$

$$\exp(-\mu_n t + \sum_{p=0}^N \frac{\Theta_{pp}}{2}t)\prod_{p=1}^N \sqrt{\frac{\pi\gamma_p}{t}}\exp\left(-\frac{(X_p - \tilde{X}_p)^2\gamma_p}{4t}\right)$$

We can conclude

$$q(X,t) = \int_{-L}^L \iint_{\mathbb{R}^N}\left(q(\tilde{X},0)\tilde{G}(X,t,\tilde{X},0) + \int_0^t \tilde{V}(\tilde{X},\tau)\tilde{G}(X,t,\tilde{X},\tau)d\tau\right)d\{\tilde{X}_p\}_{p\geq 1}d\tilde{X}_0$$

Here $\tilde{G}$ is the Green's function for q, given by

$$\tilde{G}(X,t,\tilde{X},0) = \left(\frac{1}{4\pi t}\right)^{N/2}\left(\prod_{p=1}^N \sqrt{\gamma_p}\right)\left(\sum_{n=1}^\infty \frac{B_n(X_0)B_n(\tilde{X}_0)}{\langle B_n, B_n\rangle}\exp(-\mu_n t)\right)$$

$$\exp\left(-\sum_{p=1}^N \frac{(X_p - \tilde{X}_p)^2\gamma_p}{4t} + \sum_{p=0}^N \frac{\Theta_{pp}}{2}t\right)$$

(5.3)

Moreover, $\tilde{G}(X,t,\tilde{X},\tau) = G(X,t-\tau,\tilde{X},0)$. Note that $\tilde{G}$ is symmetric under exchange of X and $\tilde{X}$.
Looking back at the p domain, we easily see

$$p(X,t) = \int_{-L}^L \iint_{\mathbb{R}^N}\left(p(\tilde{X},0)G(X,t,\tilde{X},0) + \int_0^t V(\tilde{X},\tau)G(X,t,\tilde{X},\tau)d\tau\right)d\{\tilde{X}_p\}_{p\geq 1}d\tilde{X}_0$$

Now G is given by $G = \exp(X^T H X - \tilde{X}^T H \tilde{X})\tilde{G}$. Note that the Green's function is no longer symmetric under exchange of $\tilde{X}$ an X.

5.5   Large mode displacement

A similar approximation as in the previous section could be made for large modes, where terms featuring X_0 are neglected from $(\Theta X)_p^2$. This still leaves mixed terms $X_i X_j$ where $i,j \geq 1$, and leads to particularly advanced linear algebra. Once it became clear that this approximation does not lead to an easy solution, this approximation was not further explored. Moreover, the case where the particle hardly moves, while the modes displace vigorously is not a scenario of interest.

Chapter 6

Extension to multiple compartments

For this section, we will assume that the Green's function for homogeneous Dirichlet, or absorbing, boundary conditions is given.

To truly understand the diffusion properties of the particle, we need to find its behaviour across multiple compartments, rather than within a compartment. While for multiple compartments, the partial differential equations do not satisfy absorbing boundary conditions, the Green's function for these boundary conditions can help us determine the solution to the partial differential equations.

6.1 Boundary conditions for multiple compartments

We will consider a finite linear sequence of adjacent compartments. We need boundary conditions for the places where the compartments are joined, and for the boundaries of the outer compartments. From the study of thermodynamics and diffusion, we know that fluxes, in general, are continuous, as otherwise accumulation at a point of discontinuity will appear. In this case, we similarly require continuity of probability flux. Thus if i denotes the compartment number, we have for any i:

$$-\frac{\partial p_i(X_0, t)}{\partial X_0}(L, t) - L p_i(L, t) - \sum_{l=1}^{N} \Theta_{0l} \int X_l p_i(L, \ldots, t) d(\{X_j\}_{j \geq 1})$$

$$= \frac{\partial p_{i+1}(X_0, t)}{\partial X_0}(-L, t) - L p_{i+1}(-L, t) + \sum_{l=1}^{N} \Theta_{0l} \int X_l p_{i+1}(-L, \ldots, t) d(\{X_j\}_{j \geq 1})$$

In thermodynamics and diffusion, we also see that the conserved property (heat energy and concentration respectively) is required to be continuous across the boundaries, as Fourier's law and Fick's law are only valid for a continuous conserved property. Since the probability flux as described in the previous section also has a term reminiscent of Fourier's and Fick's law, we will also require a continuous probability density. Thus:

$$p_i(L, t) = p_{i+1}(-L, t)$$

For each strand of polymer in between compartments, we then have two boundary conditions. Since these conditions are applied to two differential equations, one for each compartment, we have one condition per boundary per compartment. If we also impose a condition at each of the two outermost edges of the entire stretch of compartments, we have two boundary conditions per compartment. This is exactly the number of conditions needed for the uniqueness and existence of a solution.

What is left is now to determine boundary conditions at the outer edges. Since we expect the number of compartments chosen such that the probability density is low in the last compartment, it sounds reasonable to impose homogeneous boundary conditions at the outermost edges. Any type of homogeneous boundary conditions will do, but since the Green's function satisfies absorbing boundary conditions, we will impose these absorbing, homogeneous Dirichlet conditions at the outermost boundaries for simplicity.

6.2   Ansatz

We will write our solution p as the sum of a function p_h that satisfies the absorbing boundary conditions, and a function p_b that does not satisfy the original boundary conditions, and serves to make p satisfy the new set of boundary conditions. We will derive p_h for a given p_b, and then investigate how p_b as to be chosen.

The Fokker-Planck equation can be written as $\frac{\partial p}{\partial t} = L(p)$ for a linear operator L. This L is not concerned with the compartment size. In general we find

$$\frac{\partial p_h}{\partial t} = L(p_h) + L(p_b) - \frac{\partial p_b}{\partial t}$$

So p_h satisfies the equation with an additional source term $V = L(p_h) - \frac{\partial p_b}{\partial t}$. Using the Green's function from equation 5.3 and $G = \tilde{G} \exp(X^T H X - \tilde{X}^T H \tilde{X})$, we write

$$p_h = \int p^0(\tilde{X}) G(X, t, \tilde{X}, 0) d\tilde{X} + \int_0^t \int \left(L(p_b(\tau)) - \frac{\partial p_b}{\partial t}(\tau) \right) G(X, t - \tau, \tilde{X}) d\tilde{X} d\tau$$

We have two boundary conditions, so we will need two distinct time-dependent components, in order to control the behaviour at the boundaries. We will therefore propose

$$p_b = A(t)a + B(t)b$$

Here $A(0) = B(0) = 0$. We will now try to obtain ordinary differential equations for A and B by demanding that the boundary conditions previously described are satisfied. We then see

$$p(X, t) = A(t)a + B(t)b + \int p^0(\tilde{X}) G(X, t, \tilde{X}, 0) d\tilde{X} + \int_0^t \int \left(A(\tau) L\big(a(\tilde{X})\big) + B(\tau) L\big(b(\tilde{X})\big) \right.$$

$$\left. - \frac{\partial A}{\partial t}(\tau) a(\tilde{X}) - \frac{\partial B}{\partial t}(\tau) b(\tilde{X}) \right) G(X, t - \tau, \tilde{X}) d\tilde{X} d\tau$$

We can retrieve the marginal probability density by integrating over all modes This yields

$$p(X_0, t) = A(t) \int a \, d(\{X_j\}_{j \geq 1}) + B(t) \int b \, d(\{X_j\}_{j \geq 1}) +$$

$$\int p^0(\tilde{X}) \left(\int G(X, t, \tilde{X}, 0) d(\{X_j\}_{j \geq 1}) \right) d\tilde{X} + \int_0^t \int \left(A(\tau) L\big(a(\tilde{X})\big) + B(\tau) L\big(b(\tilde{X})\big) \right.$$

$$\left. - \frac{\partial A}{\partial t}(\tau) a(\tilde{X}) - \frac{\partial B}{\partial t}(\tau) b(\tilde{X}) \right) \left(\int G(X, t - \tau, \tilde{X}) d(\{X_j\}_{j \geq 1}) \right) d\tilde{X} d\tau$$

Due to the homogeneous Dirichlet boundary conditions of the Green's function, we find:

$$p(L, t) = A(t) \int a(L, \{X_j\}_{j \geq 1}) d(\{X_j\}_{j \geq 1}) + B(t) \int b(L, \{X_j\}_{j \geq 1}) d(\{X_j\}_{j \geq 1})$$

Through a similar argument we find

$$\sum_{l=1}^N \Theta_{0l} \int X_l p(L, \dots, t) d(\{X_j\}_{j \geq 1}) = A(t) \sum_{l=1}^N \Theta_{0l} \int X_l a(L, \dots) d(\{X_j\}_{j \geq 1}) +$$

$$B(t) \sum_{l=1}^N \Theta_{0l} \int X_l b(L, \dots) d(\{X_j\}_{j \geq 1})$$

We can also differentiate the equation for $p(X_0, t)$ to find

$$\frac{\partial p(X_0, t)}{\partial X_0} = A(t) \int \frac{\partial a}{\partial X_0} d(\{X_j\}_{j \geq 1}) + B(t) \int \frac{\partial b}{\partial X_0} d(\{X_j\}_{j \geq 1}) +$$

$$\int p^0(\tilde{X}) \int \frac{\partial}{\partial X_0} G(X, t, \tilde{X}, 0) d(\{X_j\}_{j \geq 1}) d\tilde{X} + \int_0^t \int \left(A(\tau) L(a(\tilde{X})) + B(\tau) L(b(\tilde{X})) - \right.$$

$$\left. \frac{\partial A}{\partial t}(\tau) a(\tilde{X}) - \frac{\partial B}{\partial t}(\tau) b(\tilde{X}) \right) \int \frac{\partial}{\partial X_0} G(X, t - \tau, \tilde{X}, 0) d(\{X_j\}_{j \geq 1}) d\tilde{X} d\tau$$

6.3 Adjacent compartments

We can decompose the last equation in terms such as $\int_0^t A(\tau)(\frac{\partial}{\partial X_0} \int \int L(a(\tilde{X}))G(X, t-\tau, \tilde{X}, 0)d(\{X_j\}_{j\geq 1})d\tilde{X})d\tau$. Note that this is a convolution of A with the function $(\frac{\partial}{\partial X_0} \int \int L(a(\tilde{X}))G(X, t, \tilde{X}, 0)d(\{X_j\}_{j\geq 1})d\tilde{X})$. There are three terms that that determine the probability density or probability density flux at the boundaries, these are the marginal probability density, the place derivative thereof, and the term related to expected displacement. In all three of these terms, only products of one of the functions A and B with time independent functions, and time convolutions of the functions A and B appear. We see that we will presumably not derive differential equations for A and B, but convolution equations. This is an important drawback of this method. To study these equations, we will study the Laplace transforms of the equations instead, since these convolutions then turn into multiplications. We define

$$F(X_0, \tilde{X}, s) = \mathcal{L}\{\int \frac{\partial}{\partial X_0}G(X, t, \tilde{X}, 0)d(\{X_j\}_{j\geq 1})\}$$

The transform of the probability flux can be derived from the last equations and the convolution property of the Laplace transform, and is given by

$$\mathcal{L}\{\Phi_R(p)\} = -\mathcal{L}\{A\}\left(\int \frac{\partial a}{\partial X_0}(X_0, \dots)d(\{X_j\}_{j\geq 1}) + \int L(a(\tilde{X}))F(L, \tilde{X}, s)d\tilde{X} \right.$$

$$-s\int a(\tilde{X})F(L, \tilde{X}, s)d\tilde{X} + L\int a(L, \dots)d(\{X_j\}_{j\geq 1}) + \sum_{l=1}^{N}\Theta_{0l}\int X_l a(L, \dots)d(\{X_j\}_{j\geq 1}) \right)$$

$$-\mathcal{L}\{B\}\left(\int \frac{\partial b}{\partial X_0}(L, \dots)d(\{X_j\}_{j\geq 1}) + \int L(b(\tilde{X}))F(L, \tilde{X}, s)d\tilde{X} \right.$$

$$-s\int b(\tilde{X})F(L, \tilde{X}, s)d\tilde{X} + L\int b(L, \dots)d(\{X_j\}_{j\geq 1}) + \sum_{l=1}^{N}\Theta_{0l}\int X_l b(L, \dots)d(\{X_j\}_{j\geq 1}) \right)$$

$$-\int p^0(\tilde{X})F(L, \tilde{X}, s)d\tilde{X}$$

Here Φ_R is the flux through the right side. A similar expression is found for the flux through the left-hand side. The Laplace transform for the probability at a boundary trivially follows from the equation for $p(L, t)$, and is given by:

$$\mathcal{L}\{p(L, t)\} = \mathcal{L}\{A(t)\}\int a(L, \{X_j\}_{j\geq 1})d(\{X_j\}_{j\geq 1}) + \mathcal{L}\{B(t)\}\int b(aL, \{X_j\}_{j\geq 1})d(\{X_j\}_{j\geq 1})$$

A similar expression can be obtained for the left-hand boundary It is important to note that both the probability flux and the probability at the boundary are linear functions of the Laplace transforms of A and B. From the continuity of probability flux and probability, we thus find two linear equations relating the Laplace transforms of A and B for two adjacent compartments. When the Laplace transforms of A_i and B_i are given, it is easy to compute the transforms of those functions for the next compartment.

6.4 Obtaining Laplace transforms

We now have linear equations of the Laplace transforms of the governing functions. We can say that:

$$\begin{pmatrix} A_{i+1}(s) \\ B_{i+1}(s) \end{pmatrix} = \mathcal{T}(s)\begin{pmatrix} A_i(s) \\ B_i(s) \end{pmatrix}$$

For a certain s dependent matrix $\mathcal{T}$ and compartments for which $p^0 = 0$. Typically, this will be the case for all compartments but one, since we expect to know the initial position exactly. We will assume that the compartment indices run from $-J$ to J. From the boundary conditions at the outer edges of our system, we can express $\mathcal{L}\{B\}$ in terms of $\mathcal{L}\{A\}$ for the outermost edges, and so we can express

$(A_J(s), B_J(s))^T$ in terms $A_J(s)$. By applying $\mathcal{T}(s)^{1-J}$ to this vector we get $\mathcal{L}\{A_1\}$ and $\mathcal{L}\{B_1\}$ as a function of $\mathcal{L}\{A_J\}$. We can in a similar manner determine the transforms of the governing functions in the compartment -1 of $\mathcal{L}\{A_{-J}\}$. The boundary conditions in the central compartment then give us four linear equations, allowing us to solve for the transforms A_J, A_{-J}, A_0 and B_0. Since all other transforms of A's and B's are expressed in the transform of A_J or A_{-J}, we can in this way solve for the transforms of all A's and B's.

6.5   Inverse Laplace Transforms

The question of inverting the Laplace depends largely on the Green's functions and whether these functions yield a $\mathcal{T}$ that is easily raised to a power. Eigenfunction based Green's functions form rational polynomials in s, that are conserved under matrix manipulation. These rational polynomials can be inversely transformed. This procedure is described in section 8.3.

Chapter 7

Changing boundary conditions

The main reason why we have not yet found a Green's function for our non-approximated one compartment problem is that we could not diagonalise Θ, since we cannot choose the boundary conditions for the diagonalised variables such that the solution satisfies the original boundary condition. In the last section, however, we have encountered a procedure that makes a solution satisfy certain boundary conditions, by using a Green's function for other boundary conditions. We will try to apply this procedure by diagonalising Θ and solving the problem for boundary conditions at infinity, instead of the absorbing boundary conditions at $X_0 = L$ and $X_0 = -L$. We will first look at one compartment, before diverting our attention to multiple compartments.

7.1   Method

It is easy to derive eigenfunctions for the problem when we assume the same boundary conditions for the modes and the position, as the problem can be diagonalised Suppose we have eigenfunctions f_n with corresponding eigenvalues λ_n.

We can again write our solution p as the sum of a function p_h that satisfies the original boundary conditions, and a function p_b that does not satisfy the original boundary conditions and serves to make p satisfy the new boundary conditions.

In general we find

$$\frac{\partial p_h}{\partial t} = L(p_h) + L(p_b) - \frac{\partial p_b}{\partial t}$$

So p_h satisfies the equation with an additional source term $V = L(p_h) - \frac{\partial p_b}{\partial t}$. Then we know

$$p = p_h + p_b = p_b + \sum_{n=1}^{\infty} \frac{f_n e^{-\lambda_n t}}{\langle f_n^2 \rangle} \left(\langle p^0 f_n \rangle + \int_0^t e^{\lambda_n \tau} \langle \left(L(p_b(\tau)) - \frac{\partial p_b}{\partial t} \right) B_n \rangle d\tau \right)$$

In order to make p satisfy the new boundary conditions, we have to control p_b. Since we will deal with two boundaries, we need two distinct time-dependent components in p_b. We will therefore propose

$$p_b = A(t)a + B(t)b$$

Here $A(0) = B(0) = 0$. Then

$$p = A(t)a + B(t)b+$$

$$\sum_{n=1}^{\infty} \frac{f_n e^{-\lambda_n t}}{\langle f_n^2 \rangle} \left(\langle p^0 f_n \rangle + \int_0^t e^{\lambda_n \tau} \left(A(\tau)\langle L(a)f_n \rangle + B(\tau)\langle L(b)f_n \rangle - \frac{\partial A}{\partial \tau}\langle af_n \rangle - \frac{\partial B}{\partial \tau}\langle bf_n \rangle \right) d\tau \right)$$

It is important to note that terms like $\langle L(a)f_n \rangle$ and $\langle bf_n \rangle$ are constants, only depending on n.

Looking at boundary conditions, we see that these boundary conditions typically are linear functions M of p. We will therefore study what happens when a linear function is applied to p. We again use the Laplace transform since we are dealing with convolutions.

Then

$$\mathcal{L}\{M(p)\} = \mathcal{L}\{A\}M(a) + \mathcal{L}\{B\}M(b)+$$

$$\sum_{n=1}^{\infty} \frac{M(f_n)}{\langle f_n^2 \rangle (s + \lambda_n)} (\langle p^0 f_n \rangle + \langle L(a)f_n \rangle \mathcal{L}\{A\} + \langle L(b)f_n \rangle \mathcal{L}\{B\} - \langle af_n \rangle s\mathcal{L}\{A\} - \langle bf_n \rangle s\mathcal{L}\{B\}) =$$

$$\mathcal{L}\{A\}\left(M(a) + \sum_{n=1}^{\infty} \frac{(\langle L(a)f_n \rangle - s\langle af_n \rangle)M(f_n)}{\langle f_n^2 \rangle (s + \lambda_n)} \right) + \mathcal{L}\{B\}\left(M(b) + \sum_{n=1}^{\infty} \frac{(\langle L(b)f_n \rangle - s\langle bf_n \rangle)M(f_n)}{\langle f_n^2 \rangle (s + \lambda_n)} \right) +$$

$$\sum_{n=1}^{\infty} \frac{\langle p^0 f_n \rangle M(f_n)}{\langle f_n^2 \rangle (s + \lambda_n)}$$

If we consider the case of absorbing boundary conditions, we see $M(p) = \left(\int p(L, X_1, \ldots, X_N)d\{X_j\}_{j\geq 1}, \int p(-L, X_1, \ldots, X \right.$
Then we have

$$0 = \mathcal{L}\{A\}\left(a(L) + \sum_{n=1}^{\infty} \frac{(\langle L(a)f_n \rangle - s\langle af_n \rangle)f_n(L)}{\langle f_n^2 \rangle (s + \lambda_n)} \right) + \mathcal{L}\{B\}\left(b(L) + \sum_{n=1}^{\infty} \frac{(\langle L(b)f_n \rangle - s\langle bf_n \rangle)f_n(L)}{\langle f_n^2 \rangle (s + \lambda_n)} \right) \quad (7.1)$$

$$+ \sum_{n=1}^{\infty} \frac{\langle p^0 f_n \rangle f_n(L)}{\langle f_n^2 \rangle (s + \lambda_n)}$$

Of course we have the same equation for $-L$. Here we have used $p(L)$ to denote $\int p(L, X_1, \ldots, X_N)d\{X_j\}_{j\geq 1}$.
The same notation is used for other functions, such as a and f_n

We can see that our solution will be a function of rational polynomials is s, only involving the four elementary operators. The solution will, therefore, be a rational polynomial itself. This polynomial can be simplified to a sum of terms $(s + c_i)^{-1}$ and a constant, and so the functions A and B can be recovered from the transform. This analytical process can be executed computationally, so a large number of eigenfunctions can be considered.

We can now direct our attention to the boundary conditions for multiple cells. These boundary conditions are continuous probability flux and probability at the boundaries. We will denote the probability densities as well as the functions A and B with the subscript i to denote the number of the compartment.

$$\mathcal{L}\{A_i\}\left(a(L) + \sum_{n=1}^{\infty} \frac{(\langle L(a)f_n \rangle - s\langle af_n \rangle)f_n(L)}{\langle f_n^2 \rangle (s + \lambda_n)} \right) +$$

$$\mathcal{L}\{B_i\}\left(b(L) + \sum_{n=1}^{\infty} \frac{(\langle L(b)f_n \rangle - s\langle bf_n \rangle)f_n(L)}{\langle f_n^2 \rangle (s + \lambda_n)} \right) + \sum_{n=1}^{\infty} \frac{\langle p_i^0 f_n \rangle f_n(L)}{\langle f_n^2 \rangle (s + \lambda_n)}$$

$$= \mathcal{L}\{A_{i+1}\}\left(a(-L) + \sum_{n=1}^{\infty} \frac{(\langle L(a)f_n \rangle - s\langle af_n \rangle)f_n(-L)}{\langle f_n^2 \rangle (s + \lambda_n)} \right) +$$

$$\mathcal{L}\{B_{i+1}\}\left(b(-L) + \sum_{n=1}^{\infty} \frac{(\langle L(b)f_n \rangle - s\langle bf_n \rangle)f_n(-L)}{\langle f_n^2 \rangle (s + \lambda_n)} \right) + \sum_{n=1}^{\infty} \frac{\langle p_{i+1}^0 f_n \rangle f_n(-L)}{\langle f_n^2 \rangle (s + \lambda_n)}$$

From continuous probability flux, we see as similar expression

$$\mathcal{L}\{A_i\}\left(\Phi_R(a) + \sum_{n=1}^{\infty} \frac{(\langle L(a)f_n \rangle - s\langle af_n \rangle)\Phi_R(f_n)}{\langle f_n^2 \rangle (s + \lambda_n)} \right) +$$

$$\mathcal{L}\{B_i\}\left(\Phi_R(b) + \sum_{n=1}^{\infty} \frac{(\langle L(b)f_n \rangle - s\langle bf_n \rangle)\Phi_R(f_n)}{\langle f_n^2 \rangle (s + \lambda_n)} \right) + \sum_{n=1}^{\infty} \frac{\langle p_i^0 f_n \rangle \Phi_R(f_n)}{\langle f_n^2 \rangle (s + \lambda_n)}$$

$$= -\mathcal{L}\{A_{i+1}\}\left(\Phi_L(a) + \sum_{n=1}^{\infty} \frac{(\langle L(a)f_n \rangle - s\langle af_n \rangle)\Phi_L(f_n)}{\langle f_n^2 \rangle (s + \lambda_n)} \right) -$$

$$\mathcal{L}\{B_{i+1}\}\left(\Phi_L(b) + \sum_{n=1}^{\infty} \frac{(\langle L(b)f_n \rangle - s\langle bf_n \rangle)\Phi_L(f_n)}{\langle f_n^2 \rangle (s + \lambda_n)} \right) - \sum_{n=1}^{\infty} \frac{\langle p_{i+1}^0 f_n \rangle \Phi_L(f_n)}{\langle f_n^2 \rangle (s + \lambda_n)}$$

When the Laplace transforms of A_i and B_i are given, it is easy to compute the transforms of those functions for the next compartment. This expression can then again, for a finite number of eigenfunctions, be analytically evaluated by a computer.

The method described in section 6.4 can be applied to determine the Laplace transform. The terms in the matrix $\mathcal{T}$ are rational polynomials, and so any calculation done involves an elementary operation performed on rational polynomials. When no zeros or poles are shared by two rational polynomials, any elementary operation will double the order of polynomials in the denominator and numerator. If we thus consider a moderate number of eigenfunctions, and therefore a moderate polynomial order in $\mathcal{T}$, we will still obtain rational polynomials of very large orders for $\mathcal{L}\{A\}$ and $\mathcal{L}\{B\}$, if we consider a number of compartments.

Seeing that $\mathcal{L}\{A\}$ and $\mathcal{L}\{B\}$ have to be rational polynomials, another possible method arises.

We know the basic form of $\mathcal{L}\{A_{-M}\}$, a rational polynomial. We can therefore assume a certain function $\mathcal{L}\{A_{-M}\}$, from which we calculate $\mathcal{L}\{B_{-M}\}$. We can then iteratively calculate all the transforms of the A's and B's one step at the time until we reach compartment M. The boundary condition at this compartment can then be evaluated. Repeating this process for different guesses of $\mathcal{L}\{A_{-M}\}$ in our leftmost compartment, we can find a $\mathcal{L}\{A_{-M}\}$ that will make this system suffice the rightmost boundary condition. We can then derive all original functions A and B from the transforms, and in this way also the probability density in the entire system. Since the degrees of the polynomials in $\mathcal{L}\{A_{-M}\}$ can be large, it might take numerous guesses until a satisfying $\mathcal{L}\{A_{-M}\}$ is found. The method used to retrieve the time-functions from the Laplace transforms is described in the next chapter.

7.2 Applications

The first way in which we can apply this method is, of course, to the equations dealt with in this thesis. This will be done in the next chapter. This section was however brought to be as general as possible, and we will try to describe some possible applications of this method.

This method can use the solution of a differential equation with certain boundary conditions to derive a solution satisfying different boundary conditions. In the method described above, we made use of two controlling functions, A and B, since we were dealing with a boundary condition at two points in space. This method can, of course, be extended to any finite number of boundary conditions and the same number of controlling functions. The method as described here will not work as easily when the boundary consists of an infinite number of points, such as when that boundary is a line or a plane. In that case functions like A will also have to depend on variables parametrising the boundary, rather than only on time. This will make matters much more complicated. In almost any multi-dimensional problem, we have infinite boundaries, so this method will most likely work solely for one-dimensional problems. For these problems, however, eigenfunctions can be calculated by direct integration, and not all the hassle of the method described above is necessary.

The method is therefore not as generally applicable as hoped. The question arises as to why it was effective in this situation. The main reason is that the equation is multidimensional, but that the boundary conditions are reduced to one dimension. The conditions do not depend on a specific value, but on the integral over N dimensions of the functions. This means that information is lost in these boundary conditions. Furthermore, the boundary condition includes an exotic term, which concerns expectation values of the mode displacement. This non-standard term calls for non-standard measures. This method would, therefore, be effective in other situations where the boundary conditions are not of the same dimension as the problem. So far, no such situation has been found. This does not exclude the possibility of these instances.

Chapter 8

Application of changing boundary conditions

We will now try to apply the general method described in the previous section to our problem.

8.1 Eigenfunctions

We will first derive the eigenfunctions f_n, as described in the previous section. The following equation

$$\sum_{p=0}^{N}\left(\Theta_{pp}P(X) + \sum_{i=0}^{N}\Theta_{pi}X_i\frac{\partial}{\partial X_p}P(X) + \frac{1}{\gamma_p}\frac{\partial^2}{\partial X_p^2}P(X)\right) + \lambda P(X) = 0 \tag{8.1}$$

The eigenfunctions satisfy physical boundary conditions, that is zero at infinity. From equation 2.2, the Langevin equation, we can see that a diagonal Θ gives $N+1$ independent equations, which simplifies the equation. We will try apply this diagonalisation to the Fokker-Planck equation, hoping that this will allow for separation of variables. In order to orthogonally diagonalise Θ, the matrix has to be symmetric. This means that we require $\gamma_p = 1$. The particle and the beads thus deal with the same dampening constant. For the following section, we will assume that this is true. Suppose we have an orthogonal diagonalisation

$$\Theta = M\Lambda M^{-}1 \tag{8.2}$$

Assume that $B_{n,p}$ satisfies the eigenfunction equation

$$B_{n,j}''(x) + d_j x B_{n,j}'(x) + \lambda_{n,j}B_{n,j} = 0 \tag{8.3}$$

We will substitute $P = \prod_{j=0}^{N} B_{n_j,j}((M^{-1}X)_j)$ in the eigenfunction equation for p, which is given by:

If we first divide equation 8.1 by P, and then make the substitution, we find as described in Appendix C:

$$\sum_{j=0}^{N}\frac{1 - \frac{\Lambda_{jj}}{d_j}}{B_{n_j,j}\big((M^{-1}X)_j\big)}\frac{\partial^2 B_{n_j,j}}{\partial x^2}\big((M^{-1}X)_j\big) + \lambda - \sum_{j=0}^{N}\frac{\Lambda_{jj}}{d_j}\lambda_{n_j,j} + \sum_{p=0}^{N}\Theta_{pp} = 0$$

This means that if we choose $d_j = \Lambda_{jj}$, this P is an eigenfunction with eigenvalue $\lambda = \sum_{j=0}^{N}(\lambda_{n_j,j} - \Theta_{jj})$. If we now have a bijection $l \to \mathbb{N} \to \mathbb{N}^{N+1}$, we can easily find eigenfunctions B_n with eigenvalues λ_n. Writing $l(n) = (l_1(n), \dots l_N(n))^T$, we have $B_n = \prod_{j=0}^{N} B_{l_j(n),j}((M^{-1}X)_j)$ as eigenfunctions. We know that the transformed variables $(M^{-1}X)_j$ are linearly independent. Since we have $N+1$ of these variables and $N+1$ dimensions, we see that the variables $(M^{-1}X)_j$ span $\mathbb{R}^{N+1}$. If the functions $B_{n,j}$ form a complete set on $C(\mathbb{R})$ for each j, we can therefore conclude that the eigenfunctions B_n form a complete set on $C(\mathbb{R}^{N+1})$.

We will now try to find these functions $B_{n,j}$. For moderate coupling, the eigenvalues of Θ will be determined mostly by the harmonic terms along the diagonal. Since these are all positive, we expect

the eigenvalues Λ_{jj} to be positive for moderate coupling. If we then apply the substitution $B_{n,j}(x) = \exp(-\frac{a}{2}x^2)D_{n,j}(x)$ to equation 8.3, we find

$$D''_{n,j}(x) + (\Lambda_{jj} - 2a)xD'_{n,j}(x) + a(a - \Lambda_{jj})x^2 D_{n,j}(x) + (\lambda - a)D_{n,j}(x) = 0$$

Here the substitution $d_j = \Lambda_{jj}$ has already been made. If we wish to remove the term featuring x^2, we can either choose $a = 0$, or $a = \Lambda_{jj}$. Since $a = 0$ does not change the equation at all, we choose $a = \Lambda_{jj}$ and find:

$$D''_{n,j}(x) - \Lambda_{jj}xD'_{n,j}(x) + (\lambda - \Lambda_{jj})D_{n,j}(x) = 0 \tag{8.4}$$

We see that this equation is similar to the Hermite equation[1], with the difference that this equation features $\Lambda_{jj}x$ instead of $2x$, like the Hermite equation. To rewrite this equation to the required form, we substitute $D_{n,j}(x) = \bar{D}_{n,j}(cx)$ and find

$$\bar{D}''_{n,j}(x) - \frac{\Lambda_{jj}}{c^2}x\bar{D}'_{n,j}(x) + \frac{\lambda - \Lambda_{jj}}{c^2}\bar{D}_{n,j}(x) = 0$$

Then $\frac{\Lambda_{jj}}{c^2} = 2$ gives $c = \sqrt{\Lambda_{jj}/2}$ as possible solution. Furtermore, the equation is then solved by $\bar{D}_{n,j} = H_n(x)$, with $\frac{\lambda - \Lambda_{jj}}{c^2} = 2n$. H_n here is the n'th physicist's Hermite equation. Equation 8.3 is then solved by $B_{n,j}(x) = \exp(-\frac{\Lambda_{jj}}{2}x^2)H_n(x\sqrt{\Lambda_{jj}/2})$ with eigenvalues $\lambda_n = \Lambda_{jj}(n+1)$. Note that $\lim_{x\to\pm\infty} B_{n,j}(x) = 0$ as required. Furthermore, the Hermite polynomials form a complete set on $C(\mathbb{R})$. As a result the functions $B_{n,j}$ are complete set on $C(\mathbb{R})$ and thus the functions satisfying the ansatz $P = \prod_{j=0}^{N} B_{n_j,j}((M^{-1}X)_j)$ form a complete set on $C(\mathbb{R}^{N+1})$ as explained above. We conclude that the solutions of equation 4.1 with physical boundary conditions at infinity are given by

$$p(X,t) = \sum_{n=1}^{\infty} c_n \left(\prod_{j=0}^{N} \exp(-\frac{\Lambda_{jj}}{2}x^2) H_{l_j(n)}\left((M^{-1}X)_j\sqrt{\Lambda_{jj}/2}\right) \right) \exp(-\sum_{j=0}^{N} \lambda_{l_j(n)}t)$$

8.2   Implications of negative eigenvalues

In the derivation of the eigenfunctions of equation 4.1, it was assumed that Θ only has positive eigenvalues. While this assumption is not a strange assumption, it is worthwile to investigate the case of a negative eigenvalue of Θ. Equation 8.3 for a negative value of $d_j = \Lambda_{jj}$, is similar to equation 8.4 and can in a similar manner be shown to yield Hermite polynomials as result. All Hermite polynomials but the first, divert to plus or minus infinity for infinite $|x|$. Moreover the time evolution of this eigenfunction is $\exp(-\Lambda_{jj}t) = \exp(|\Lambda_{jj}|t)$.

This means that the probability density becomes larger for values far from the origin and increases in time for this eigenfunction. This would imply that if there is a negative eigenvalue Λ_{jj} such that $(M^{-1})_{j0} \neq 0$, we would see that with increasing time, the probability density becomes small at the initial position while it would become increasingly large for positions further from the origin. This can be interpreted as a particle that does not diffuse in a random manner but is actively steered to the sides.

In the previous section it was argued that negative values would not occur for situations with small coupling. The described behaviour of a particle being pushed to the sides is therefore only possible for situations with larger coupling. This is all in line with the predictions made in section 3.3, which said that for large coupling, particles are super-ballistically pushed to either the right or the left side.

In section 3.3, it was also argued that this behaviour is not in line with the expected physical behaviour and that this model can only be applied to situations where the coupling is not too large compared to the harmonic forces. We can now specify this criterion of being too large, by demanding that Θ has no negative eigenvalues. In all simulations presented in this thesis, s_1 was kept low enough to ensure that this criterion was met, except when explicitly stated. The demand of only positive eigenvalues is a major restriction on the model presented in this thesis.

8.3   Computation of controlling functions

This section will present how the method in the previous section is implemented. A Matlab script was used for the evaluation of certain integrals, and to perform algebraic operations on rational polynomials.

This script is included in Appendix E. These operations are done through analytical means, rather than by simulations of any kind. We have first applied the method to obtain a solution to the equation with absorbing boundary conditions, limiting ourselves to one compartment. For the sake of easy programming, only one mode was considered at first. Furthermore, $a(X) = X_0 \exp(-K_1 X_1^2)$ and $b(X) = \exp(-K_1 X_1^2)$ were chosen as they are the most elementary functions in X_0, multiplied by the factor $\exp(-K_1 X_1^2)$ which ensures that this function is integrable along the X_1 direction.

Equation 7.1 linearly relates $\mathcal{L}\{A\}$, $\mathcal{L}\{B\}$ and the initial condition, in order to satisfy zero probability at L. A similar relation can be obtained for $-L$. This yields the matrix equation

$$\begin{pmatrix} \Pi_{11}(s) & \Pi_{12}(s) \\ \Pi_{21}(s) & \Pi_{22}(s) \end{pmatrix} \begin{pmatrix} \mathcal{L}\{A\}(s) \\ \mathcal{L}\{B\}(s) \end{pmatrix} = \begin{pmatrix} e(s) \\ f(s) \end{pmatrix}$$

Here Π_{ij}, e and f are all given by $c_0 + \sum_{n=1}^{\infty} \frac{c_n}{s+\lambda_n}$ for different sets of coefficients $\{c_n\}$. Only a finite number eigenvalues were considered, which means that all terms in the matrix equation can be written as a rational polynomial. It was chosen to use just 5 eigenfunctions at first. Since the inverse of a 2-dimensional matrix can be directly calculated with basic elementary operations, Π can be inverted with s as a parameter. The elements of Π^{-1} are then again given as rational polynomials. Multiplying Π^{-1} with $(e(s), f(s))^T$ gives $\mathcal{L}\{A\}(s)$ and $\mathcal{L}\{B\}(s)$ as rational polynomials. Any zero-pole pairs resulting from the fact that all terms in the matrix equation have the same poles were eliminated, and consequently, the functions A and B were calculated from their Laplace transforms.

In order to do this, it was noted that rational polynomials like $\mathcal{L}\{A\}$ can be written as a sum of terms $d_n/(s - p_n)$, where p_n are the poles of $\mathcal{L}\{A\}$. The coefficients d_n are related through a matrix equation. Since $\mathcal{L}\{d_n \exp(p_n t)\} = d_n/(s - p_n)$, this partial fraction expansion directly yield the time-functions belonging to the Laplace transforms. While no 2 poles lay especially close to each other, the matrix turned out to be highly singular, with condition numbers of about 10^{-19}, and three-quarters of the eigenvalues approximately zero. Changes in parameters did not help this problem, so the high singularity is definitely not chance. A reason for this high singularity was not found since the poles were not that close to each other.

If this problem is solved, the last hurdle is taken in solving this model one compartment, and an attempt can be made at solving the model for multiple compartments. If this is the case, it means that a solvable model is found. Since no such model is present as of yet, this could be an interesting development, especially if the accuracy of the model is further explored. For now, the method cannot be applied.

The intention was to apply this method to solve for multiple compartments after doing this for one compartment, but since that step proved not possible, the final step of multiple compartments has been made.

Chapter 9

Results approximation of Fokker-Planck equation

In section 5.4, an approximation was described in the case of small Rouse mode displacement. A Green's function to the modified equation was also presented. Using this Green's function, the marginal probability density in X_0 was determined for initial conditions of a Dirac delta function at $X_0 = 0$. No sources were considered. The total probability density in the compartment, or the chance of the particle being in the compartment, is displayed in figure 9.1. The parameters used were $N = 10, L = 1, K_1 = 1, \gamma = 1$ and $s_1 = 0.1$, and 11 eigenfunctions were considered.
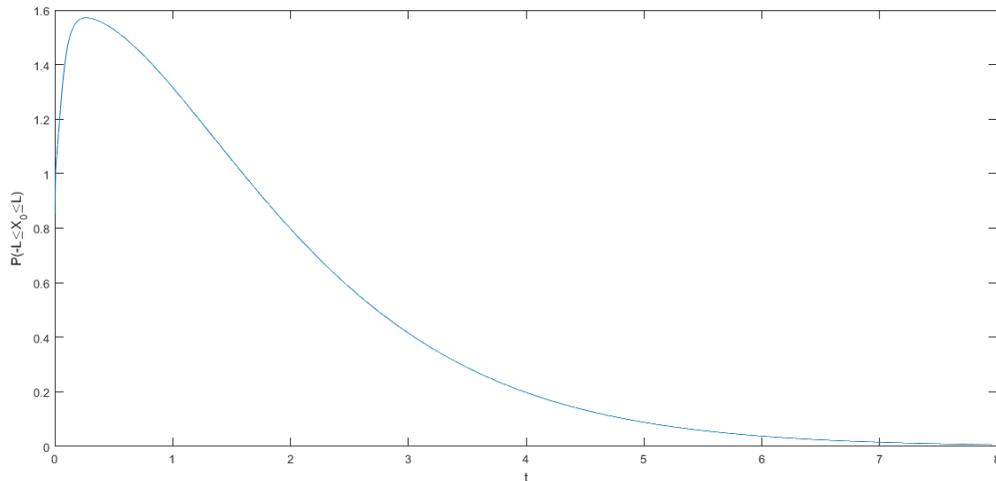
Figure 9.1: The probability of the particle being in the initial compartment when initially at the centre, according to the small mode displacement. $N = 10, L = 1, \gamma = 1$ and $s_1 = 0.1$

It is clear that the curve in the figure is not what one would expect, as the probability obtains values of over 1.5, which is of course not physically possible. The parameter domain is algorithmically searched for parameters that do not yield probabilities larger than 1, and those parameter combinations have not been found. For any parameter choice studied, probabilities significantly higher than 1 were found.

In section 5.4 it was found that the approximation adds a term $p(X,t)\Big(\sum_{p=0}^{N} \frac{\gamma_p}{4} \big((\sum_{j=0}^{N} \Theta_{pj} X_j)^2 - \Theta_{p0} X_0^2 \big) \Big)$ to $\frac{\partial p}{\partial t}$. This term is always positive and therefore it is not surprising that the probability becomes larger than it should. It is, of course, a shame that the magnitude of this increase is such that non-physical results are obtained.

Since this approximation yields results which are clearly not close to the truth, it becomes clear that true cases of small mode displacement cannot be found. The principal way in which mode displacements

can be kept small is by increasing the harmonic constants K_p. The problem is that the approximation does not necessarily hold when the mode displacement X_j is small, but when $p(X,t)\Big(\sum_{p=0}^{N}\frac{\gamma_p}{4}\big((\sum_{j=0}^{N}\Theta_{pj}X_j)^2-\Theta_{p0}X_0^2\big)\Big)$ is small. This means that $\Theta_{pj}X_j$ is small for all values p and j, and that thus K_jX_j is small. This term is minus the harmonic force on the mode. The harmonic force competes with thermal noise, so when the harmonic force stays of constant magnitude, typical values of K_jX_j will also remain equally large. Large values of K_j cannot make the mode displacement small, as in reality K_jX_j has to be made small.

We can see that a smaller noise term can also decrease typical mode displacement. Small noise can be obtained by a large value of γ since the noise on the modes scales inversely with γ. We however also see that $p(X,t)\Big(\sum_{p=0}^{N}\frac{\gamma_p}{4}\big((\sum_{j=0}^{N}\Theta_{pj}X_j)^2-\Theta_{p0}X_0^2\big)\Big)$ scales with γ. This cancels the effect of a lower mode displacement.

We can conclude that although the approximation made in section 5.4 generate an analytically derivable Green's function, the conditions for the approximation to hold cannot be satisfied. This further increase the need for an exact solution as described in section 8.

Chapter 10

Verification of predicitions

In section 3, a few predictions have been made concerning α. In this section, these will be tested using simulations. These simulations were made using the forward Euler method since it is the simplest method for these types of simulations. Implicit methods such as backward Euler are not viable options due to the non-continuous nature of the force a particle experience across the boundaries. The equation that needs to be solved each time-step can have multiple solutions, as the particle can be in two different compartments at the end of each time step. Other more complex methods such as the Runge-Kutta method might also experience such problems, and it was chosen to dedicate time to obtaining analytical solutions, rather than study the application of methods like Runge-Kutta to this non-continuous and stochastic process. It is also worth noticing certain methods are advantageous over forward Euler, mostly because they decrease the number of time-steps needed. Using less time-steps means that fewer evaluations of the stochastic variable Ξ are made per simulation. These methods thus call for a larger number of simulations, in order to make an equally accurate result. Every time a variance was computed, 500 realisations were used since this number found a balance between speed and accuracy. The Matlab script used is included in Appendix D When a particle crossed a boundary, the mode displacements were set to zero, to express that it is unknown how mode displacements in different compartments are related. Generally, we have used $K_p = K_1 p^{-\alpha}$ where $\alpha = 1 + 2\nu$ and ν is the Flory exponent [3]. We assume a similar structure for s_p.

10.1 Large times

It was predicted that for large times, regular diffusion will take place, implying an α of 1. All simulations done have verified that for timescales in which most particles have switched compartments a number of times, the diffusion is indeed linear. Plots of these simulations will not be particularly enlightening to the reader and are therefore not included.

10.2 Small times, small coupling

When the harmonic force is dominant over the coupling force, it was predicted that initially, regular diffusion will take place. For infinitely large compartments the variance will reach an equilibrium value. If L^2 is much higher than this equilibrium variance, we expect that for relatively short times, the initial regular diffusion will change into a constant variance. If L^2 is much lower than the equilibrium variance, the initial regular diffusion is still present when the particles cross the first polymer strand. At this point, the particle will experience regular diffusion since we are dealing with the large time regime. We will thus get regular diffusion across the entire time domain. For values of L^2 closer to the equilibrium variance, things can get more interesting. It is not clear what values of L^2 form the difference between these two length scales, only that they will be of the order of magnitude of the equilibrium variance. Simulations have been made for a range of values of L. Here $N = 10$, $\gamma_p = 1$, $K_1 = 1$ and $s_1 = 0.1$. s_1 has deliberately been chosen low, to ensure that the coupling is indeed small. These simulations can be found in figure 10.1. The final variance decreases as L increases, and the equilibrium variance is found to approximately 2. The first prediction made, was that for short L regular diffusion would occur, and that no anomalous
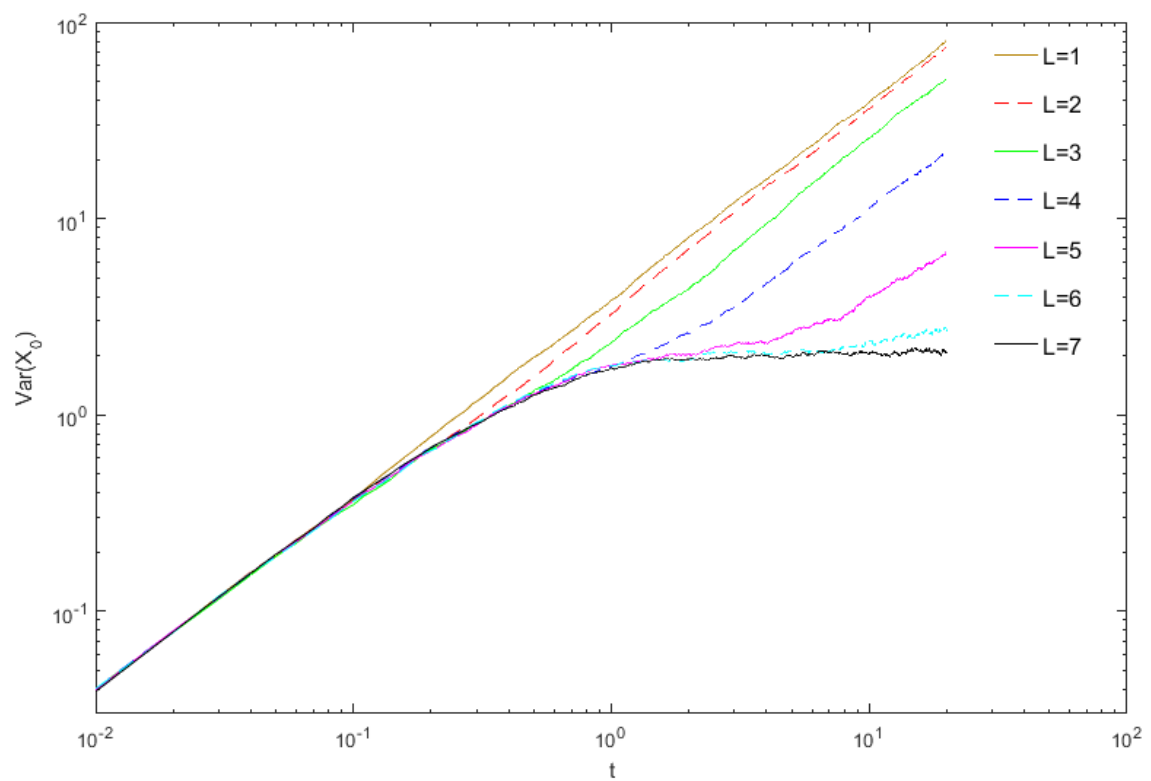
Figure 10.1: Plot of variance for different values of L. The final variance is largest for low values of L. Sub-diffusion is evident around the equilibrium variance. Here $N = 10$, $K_1 = 1$, $\gamma = 1$ and $s_1 = 0.1$

behaviour will take place. This is supported by figure 10.1, where we clearly see that for $L = 1$ regular diffusion occurs. It is worthwhile to note that the deviation from regular diffusion is smaller for small values of L^2.

Next, it was predicted that a plateau would be reached for large values of L. It is clear that such as plateau is reached for $L = 7$ and $L = 6$. For $L = 6$, the variance is just leaving the plateau within this time scale, while for $L = 7$, the plateau will only be departed for longer times. At first, regular diffusion occurs, but as the variance approaches the equilibrium variance, diffusion slowly stops and α becomes 0. The values of L^2 of 36 and 47 are significantly larger than the equilibrium variance of around 2 as required.

The last regime the predictions tackled in the section 3.2 was the regime with values of L^2 not significantly larger nor smaller than the equilibrium variance. No concrete predictions could be made for this regime other than that it would be a mixture of the two regimes.

It is clear that initially, the variances follow the curve of $L = 7$, the curve with the plateau. Each curve leave the plateaued curve at some point in time, from where they will continue to diffuse with $\alpha = 1$. The larger L, the later this point. The $L = 1$ curve leaves the plateaued curve as soon as the $L = 7$ curve starts to show sub-diffusion, while the $L = 6$ curve only leaves the plateaued curve after that plateau has been reached.

Considering that for example L^2 for $L = 3$ is more than four times as large as the equilibrium variance, and that the deviation from regular diffusion is rather small for that value of L, we can conclude that rather large compartments are required to experience some form of anomalous diffusion. Furthermore, for every value of L, sub-diffusion only occurs on a limited time range. For both large and short times, regular diffusion is always found.

We can conclude the sub-diffusion is possible in this model, but that this is only present for specific situations, and only happens during the transition from the particles being in the first compartment to them being in the next.

10.3 Small times, large coupling

In section 3, it was argued that remarkable behaviour will take place when the coupling dominant over the particle's harmonic potential. The particle could super-ballistically move towards a polymer strand. To verify this, simulations have been made with a range of values for s_1 and $L = 1$, $K_1 = 1$ and $\gamma = 1$. A simulation has also been made for an infinite compartment, enabling the study of the development of α over time.

From figure 10.2, we can see that for large values of s_1, the particle "diffuses" at enormous rates, with α's of 4.5 for $s_1 = 1000$. This super-ballistic diffusion stops at a variance of 1, which is equal to L^2. This confirms the prediction from section 3.3 that read that particles would quickly move to either the left or right-hand polymer, where they would be trapped.

It was predicted that once this variance of L^2 was reached, regular diffusion would occur, as particles now diffuse from polymer strand to polymer strand. This is not visible in figure 10.2, most probably because this does not happen on the time scale studied. To best visualise the diffusion from a polymer strand, the particles are now at $X_0 = L$ for $t = 0$, rather than at $X_0 = 0$. In figure 10.3 we can see that linear diffusion indeed holds for smaller values of s_1, but that for $s_1 = 100$, further diffusion is not found in this time scale. A similar situation occurs as in for small coupling, where the particle displacement reaches an equilibrium variance. This equilibrium variance happens to be far lower that the inter-polymer distance, so diffusion does not take place. It is expected that for very large timescales, diffusion will eventually take place. This is not simulated, due to computational limitations.

In section 8.2, it was claimed that this super-diffusive behaviour takes place for all values of s_1 for which Θ has negative eigenvalues. From the values of s_1 plotted in figure 10.2, all values of s_1 but $s_1 = 0.1$ yield at least one negative eigenvalue, but super-diffusion is not visible for all these values. When super-diffusion does occur, it takes time for this effect to start, and it is, therefore, reasonable to assume that by the time a process with for example $s_1 = 1$ could start this super-diffusion, a variance of L^2 has already been reached. To verify whether even relatively low values of s_1 that yield negative eigenvalues cause super-diffusion or even super-ballistic motion, we will simulate this process for an infinite L. In this way, there is ample time for super-diffusion to develop. This simulation is visualised in figure 10.4. It is clear that the even in a log-log plot, the variance shows an exponential curve, reaching $\alpha = 22$ for $s_1 = 1$.
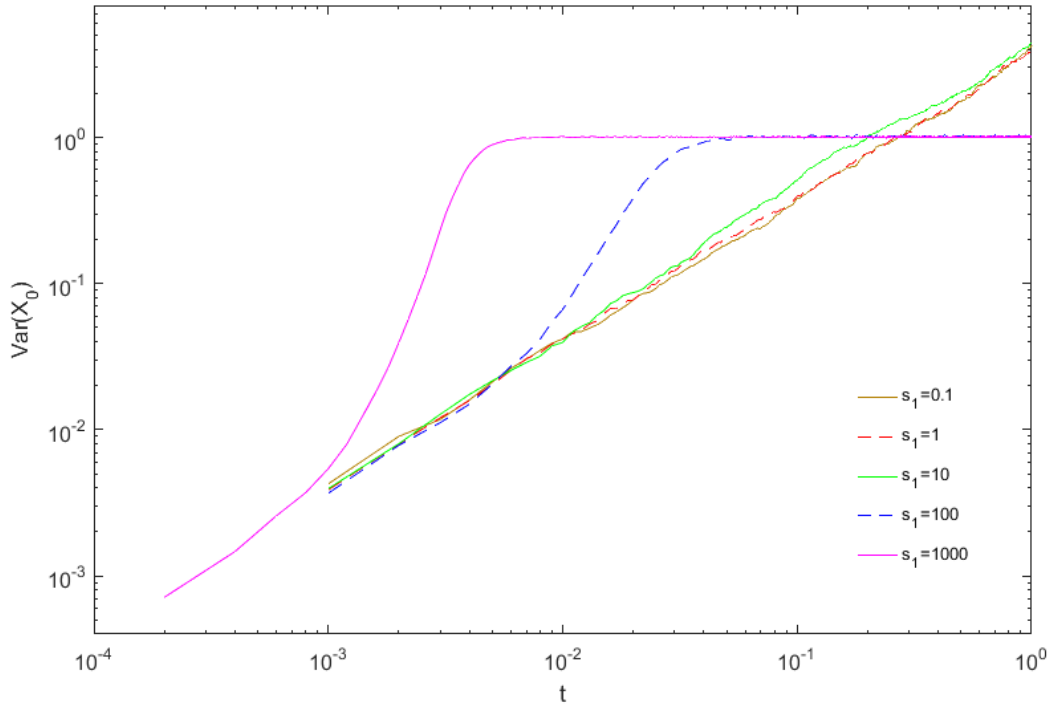
Figure 10.2: The variance of the particle position plotted for $L = 1$, $K_1 = 1$, $\gamma = 1$ and various values of s_1. $s_1 = 1000$ has been plotted with a finer time scale, since this was required to obtain accurate simulations

This means that α increases indefinitely, even for relatively small values of s_1 where only one eigenvalue is negative.

A similar simulation was also made for $s_1 = 0.1$ where all eigenvalues were positive, and it turned out that even on large timescales, super-diffusion did not occur, as visible in figure 10.5. In this figure, it is clear that variance increases linearly with time until an equilibrium variance is reached. We can conclude that the condition of no negative eigenvalues is a sharp rule rather than an order of magnitude guess.
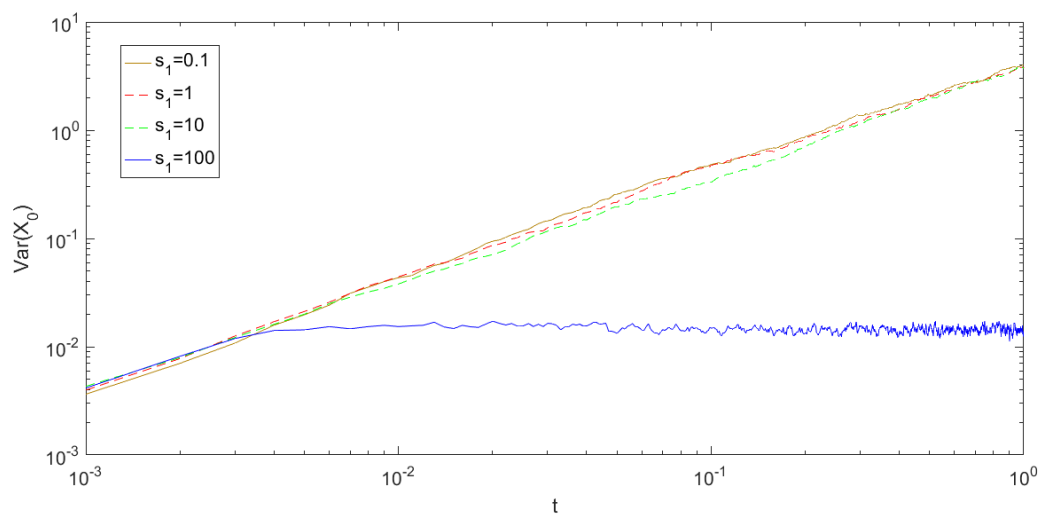
Figure 10.3: Plot of the variance of the particle position for $L = 1$, $\gamma = 1$, $K_1 = 1$ and a range of values s_1
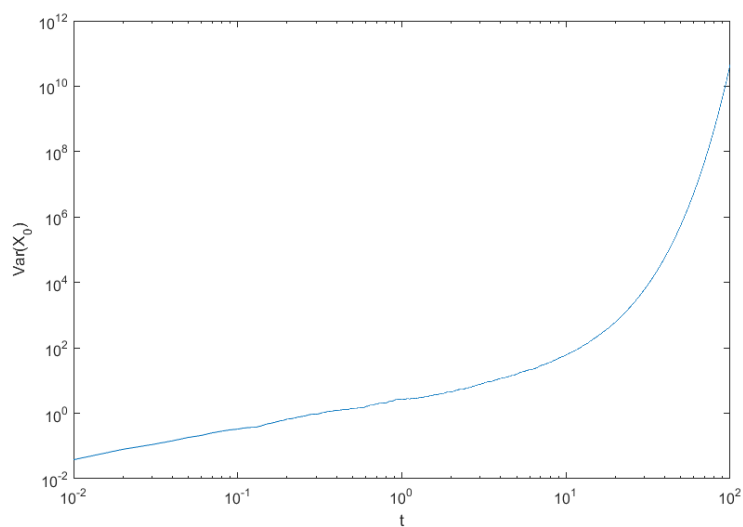
Figure 10.4: Plot of the variance of the particle position for an infinite compartment, with $L = 1$, $\gamma = 1$, $K_1 = 1$ and $s_1 = 1$. Super-diffusion is clearly visible
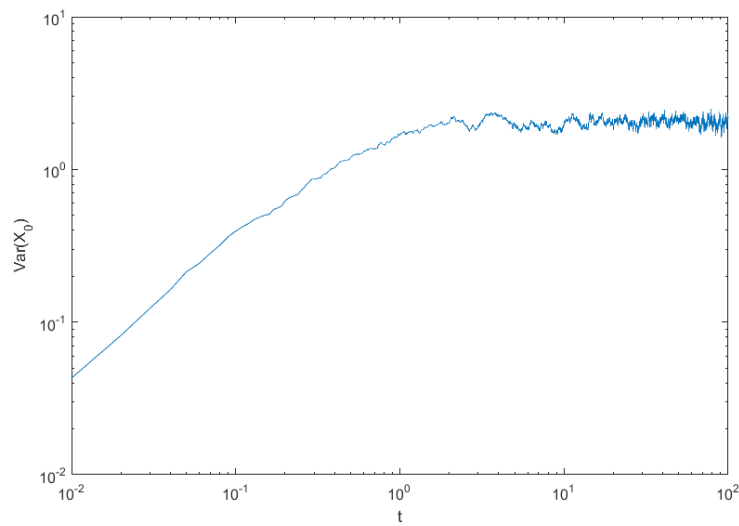
Figure 10.5: Plot of variance of particle position for an infinite compartment, with $L = 1$, $\gamma = 1$, $K_1 = 1$ and $s_1 = 0.1$. It is clear that the variance reaches a plateau

Chapter 11

Effects of polymer concentration

The previous chapter dealt mostly with α, and while the power of diffusion is more interesting that the diffusion speed D, we will still quickly study this variable. In enviroments with high concentration of polymers, D is seen to behave as $D \propto \exp(-vc)$ [8]. Here v is some constant, and c is the percentual concentration of polymers. We would thus expect that in this model $D \propto \exp(-v'\bar{L}^{-1})$ or $D \propto \exp(-v'\bar{L}^{-3})$. We will test our model with this empirical paper, by simulating this experiment.

We would like to choose parameters by which we vary $\bar{L}$ and keep all other factors constant. Since we want the maximum potential values to be constants for varying $\bar{L}$, we see that $\bar{K}_0 \propto \bar{L}^{-2}$ and that $\bar{S}_1 \propto \bar{L}^{-1}$. The dimensionless variables L and γ remain constant under this varying concentration, while $K_1 \propto \bar{L}^2$ and $S_1 \propto \bar{L}$. Simulations were carried out over a range of values of $\bar{L}$. The parameters were chosen such, that for $\bar{L} = 1$, we have $L = 1$, $\gamma = 1$, $K_1 = 1$ and $s_1 = 0.1$. The other parameters scale as described above. The specific values of $\bar{L}$ are irrelevant, only the dimensionless quantities assigned to those values of $\bar{L}$. A linear timescale was used with a maximum time of 5 and 10000 time steps. This lead to figure 11.1. If this model complies with the experimental results, we should see a straight line with a downward slope, since the vertical axis has a logarithmic scale.
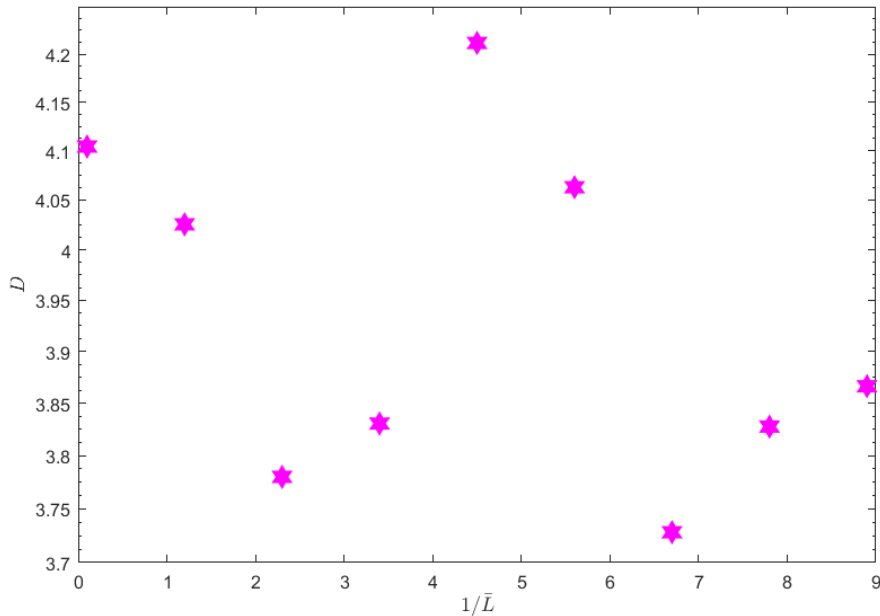
Figure 11.1: Diffusion coefficient for a range of compartment lengths, with a linear scale for the horizontal axis and a logarithmic scale for the vertical axis. Here $L = 1$, $\gamma = 1$, $K_1 = 1$ and $s_1 = 0.1$ for $\bar{L} = 1$,

It is clear that on this variable range, no clear relation between the coefficients can be observed. It is

unclear whether the x-axis should display $\bar{L}^{-1}$ or $\bar{L}^{-3}$, however we can see that changing the x-axis will not create a logical result. It is therefore natural to conclude that this model does not satisfy the same relation as is observed in practice. It is, however, noteworthy that based on the experimental study, we expect a clear relation for concentrations in the order of 50%, while the difference between a concentration of 0.1% and 0.2% will not be as clear. Not observing a clear relation could therefore also hint at not finding the right range of values of $\bar{L}$. The range displayed is not the only range tested, and no relation was found for any range.

Chapter 12

Conclusion

The goal of this thesis was to describe a model, test it for accuracy and solve the model.

Right after the model was presented, predictions have been made about the expected behaviour of the model. It was found that the model can describe anomalous diffusion on a relatively short time scale, the scale where particles are just crossing the first polymer. Anomalous diffusion on a longer time scale was clearly not a possible result, which means that the model cannot explain anomalous diffusion over lengths of more than the polymer separation. Furthermore, it was found that for certain parameter regimes, super-ballistic motion was possible. Since super-ballistic motion is obviously not something a diffusing particle would likely experience, it became clear that the relevant parameter regime is not a regime that can be taken seriously for this model. Later a criterion was developed to test whether a certain parameter combination can be applied to this model. This unexpected behaviour is a reason to become weary of the model.

Later, the Fokker-Planck equation of this model was studied and certain approximations were explored. One approximation was the small-mode displacement approximation, which proved solvable, and so a Green's function was obtained. It became however clear that for every parameter choice, probability was not conserved, and that the total probability increased with time. Closer study of the made approximation showed that the conditions for the approximations cannot be satisfied by any parameter choice.

Next, the problem of multiple compartments was studied, and it was reasoned that the model requires continuous probability flux and continuous probability across the boundaries of the compartments. In order to impose these boundary conditions on the equations, the probability density was written as the sum of a function that satisfied homogeneous Dirichlet boundary conditions, and two other functions that could be controlled in order to make sure that the sum of these three functions satisfied the appropriate boundary conditions. The impact of the controlling functions was described as a source term, enabling the use of the Green's function for homogeneous Dirichlet boundary conditions. The controlling functions necessary to make the probability density satisfy the right boundary conditions were found to satisfy a certain convolution equation. From this equation, the Laplace transforms and eventually the controlling functions could be retrieved. This method could not easily be tested since no Green's function satisfying the right boundary conditions was available.

The method of adding functions to a function with certain boundary conditions to change those boundary conditions was then made more generally applicable and was able to derive an analytic solution to the Fokker-Planck equation with homogeneous boundary conditions. This solution would be a solution to the original, non-approximated equation. It was also shown how the method could be applied to the problem of a long stretch of compartments. When applying this method, far along in the process of applying the method, a highly singular matrix had to be inverted in order to invert a Laplace transform, thus disabling the possibility of an accurate result. The cause of this high singularity is not found and is a problem worth further study, since solving that problem would mean a solution to the set of equations.

The main objective of this thesis was to describe, test and solve a model. The model made is for the largest part intuitive, while the coupling between polymers and the particle was no more than a guess. The coupling proved to lead to strange effects such as super-ballistic diffusion for certain parameter regimes. Although this behaviour was not present for most parameter choices, the presence of these anomalies is a good argument against the accuracy of this model. The model proved not even easy to solve since it features an array of partial differential equations, which are not easily solved on themselves.

Connecting different partial differential equations also created difficulties. Despite these difficulties, a method of solving the problem was obtained, which experienced certain practical difficulties. Should these issues be resolved, we have a model that somewhat describes the problem, otherwise, we are stuck with an unsolvable model with some undesired properties.

Appendix A

Marginal probability density

We will repeatedly integrate the differential equation for p to determine the time derivative of the marginal probability density of p.

Define I_n as p integrated over all modes $N + 1 - n \leq p \leq N$. Note that $I_0 = p$. Assume

$$\frac{\partial I_k}{\partial t} = \sum_{p=0}^{N-k} \Theta_{pp} I_k + \sum_{p=0}^{N-k} (\sum_{i=0}^{N-k} \Theta_{pi} X_i) \frac{\partial I_k}{\partial X_p} + \sum_{p=0}^{N-k} \frac{1}{\gamma_p} \frac{\partial^2 I_k}{\partial X_p^2} + \sum_{p=0}^{N-k} (\sum_{i=N-k+1}^{N} \Theta_{pi} \frac{\partial}{\partial X_p} \int X_i p(X,t) d(\{X_j\}_{j \geq N-k+1}))$$

for some k. Then we find,

$$\frac{\partial I_{k+1}}{\partial t} = \int_{-\infty}^{\infty} \frac{\partial I_k}{\partial t} dX_{N-k}$$

$$= \sum_{p=0}^{N-k} \Theta_{pp} I_{k+1} + \sum_{p=0}^{N-(k+1)} (\sum_{i=0}^{N-(k+1)} \Theta_{pi} X_i) \frac{\partial I_{k+1}}{\partial X_p} + (\sum_{i=0}^{N-(k+1)} \Theta_{(N-k),i} X_i) \int_{-\infty}^{\infty} \frac{\partial I_k}{\partial X_{N-k}} dX_{N-k} +$$

$$\sum_{p=0}^{N-(k+1)} \Theta_{p,(N-k)} \frac{\partial}{\partial X_p} \int_{-\infty}^{\infty} X_{N-k} I_k dX_{N-k} + \Theta_{(N-k),(N-k)} \int_{-\infty}^{\infty} X_{N_k} \frac{\partial I_k}{\partial X_{N-k}} dX_{N-k} + \sum_{p=0}^{N-(k+1)} \frac{1}{\gamma_p} \frac{\partial^2 I_{k+1}}{\partial X_p^2}$$

$$+ \frac{1}{\gamma_{N-k}} \int_{\infty}^{\infty} \frac{\partial^2 I_k}{\partial X_{N-k}^2} dX_{N-k} + \sum_{p=0}^{N-(k+1)} (\sum_{i=N-k+1}^{N} \Theta_{pi} \frac{\partial}{\partial X_p} \int X_i p(X,t) d(\{X_j\}_{j \geq N-k}))$$

$$+ \sum_{i=N-k+1}^{N} \Theta_{(N-k).i} \int_{-\infty}^{\infty} \frac{\partial}{\partial X_{N-k}} \int X_i p(X,t) d(\{X_j\}_{j \geq N-k+1}) dX_{N-k}$$

$$= \sum_{p=0}^{N-k} \Theta_{pp} I_{k+1} + \sum_{p=0}^{N-(k+1)} (\sum_{i=0}^{N-(k+1)} \Theta_{pi} X_i) \frac{\partial I_{k+1}}{\partial X_p} + \Theta_{(N-k),(N-k)} (X_{N-k} I_k |_{-\infty}^{\infty} - I_{k+1})$$

$$+ \sum_{p=0}^{N-(k+1)} \frac{1}{\gamma_p} \frac{\partial^2 I_{k+1}}{\partial X_p^2} + \sum_{p=0}^{N-(k+1)} (\sum_{i=N-k}^{N} \Theta_{pi} \frac{\partial}{\partial X_p} \int X_i p(X,t) d(\{X_j\}_{j \geq N-k}))$$

$$= \sum_{p=0}^{N-(k+1)} \Theta_{pp} I_{k+1} + \sum_{p=0}^{N-(k+1)} (\sum_{i=0}^{N-(k+1)} \Theta_{pi} X_i) \frac{\partial I_{k+1}}{\partial X_p} + \sum_{p=0}^{N-(k+1)} \frac{1}{\gamma_p} \frac{\partial^2 I_{k+1}}{\partial X_p^2}$$

$$+ \sum_{p=0}^{N-(k+1)} (\sum_{i=N-k}^{N} \Theta_{pi} \frac{\partial}{\partial X_p} \int X_i p(X,t) d(\{X_j\}_{j \geq N-k}))$$

This is the initial assumption evaluated in $k + 1$. Since this assumption for $k = 0$ is equivalent to the main differential equation, it follows from mathematical induction that this assumption is valid for all k. Note that I_N is the marginal probability distribution $p(X_0, t)$ of $p(X, t)$ in X_0 and that

$$\frac{\partial p(X_0, t)}{\partial t} = \frac{\partial I_N}{\partial t} = \Theta_{00} p(X_0, t) + \Theta_{00} X_0 \frac{\partial p(X_0, t)}{\partial X_0} + \frac{\partial^2 p(X_0, t)}{\partial X_0^2} + \frac{\partial}{\partial X_0} \sum_{i=1}^{N} \Theta_{0i} \int X_i p(X, t) d(\{X_j\}_{j \geq 1})$$

Appendix B

Analogous representation

In order to make sure that separation of variables can be used for P, we evaluate $p(X) = q(X)exp(X^THX)$, for some $(N+1) \times (N+1)$ matrix H. We then find

$$\frac{\partial}{\partial X_i}X^THX = \sum_{j=0}^{N}(H_{ij} + H_{ji})X_j$$

And therefore

$$\frac{\partial p(X)}{\partial X_i} = \exp(X^THX)(\frac{\partial q(X)}{\partial X_i} + q(X)\sum_{j=0}^{N}(H_{ij} + H_{ji})X_j)$$

Furthermore

$$\frac{\partial^2 p(X)}{\partial X_i^2} = \exp(X^THX)(\frac{\partial^2 q(X)}{\partial X_i^2} + 2\frac{\partial q(X)}{\partial X_i}\sum_{j=0}^{N}(H_{ij} + H_{ji})X_j + q(X)((\sum_{j=0}^{N}(H_{ij} + H_{ji})X_j)^2 + 2H_{ii}))$$

Then

$$\frac{\partial q}{\partial t} = \sum_{p=0}^{N}(\frac{\partial^2 q(X)}{\partial X_p^2}\frac{1}{\gamma_p} + \frac{\partial q(X)}{\partial X_i}\sum_{j=0}^{N}(\frac{2}{\gamma_p}(H_{pj} + H_{jp}) + \Theta_{pj})X_j$$

$$+Q(X)((\sum_{j=0}^{N}(H_{pj} + H_{jp})X_j)(\sum_{j=0}^{N}(\frac{1}{\gamma_p}(H_{pj} + H_{jp}) + \Theta_{pj})X_j) + \frac{2}{\gamma_p}H_{pp} + \Theta_{pp}))$$

Appendix C

Substitution of P

Making the substitution as described in section 8, we find

$$\sum_{p=0}^{N} \Theta_{pp} + \sum_{p=0}^{N} \sum_{i=0}^{N} \Theta_{pi} X_i \sum_{j=0}^{N} \frac{M_{jp}^{-1}}{B_{n_j,j}((M^{-1}X)_j)} \frac{\partial B_{n_j,j}}{\partial x}((M^{-1}X)_j)+$$

$$\sum_{p=0}^{N} \frac{1}{\gamma_p} \sum_{j=0}^{N} \frac{(M_{jp}^{-1})^2}{B_{n_j,j}((M^{-1}X)_j)} \frac{\partial^2 B_{n_j,j}}{\partial x^2}((M^{-1}X)_j)+$$

$$2\sum_{p=0}^{N} \sum_{j=0}^{N} \sum_{l \neq j} \frac{M_{jp}^{-1}}{B_{n_j,j}((M^{-1}X)_j)} \frac{\partial B_{n_j,j}}{\partial x}((M^{-1}X)_j) \frac{M_{lp}^{-1}}{B_{n_l,l}((M^{-1}X)_l)} \frac{\partial B_{n_l,l}}{\partial x}((M^{-1}X)_l)M_{lp}^{-1} + \lambda = 0$$

Looking at the second term we see:

$$\sum_{i=0}^{N} \sum_{p=0}^{N} M_{jp}^{-1} \Theta_{pi} X_i = \sum_{i=0}^{N} (M^{-1}\Theta)_{ji}(MM^{-1}X)_i = (M^{-1}\Theta M M^{-1}X)_j = (\Lambda M^{-1}X)_j = \Lambda_{jj}(M^{-1}X)_j$$

And thus:

$$\sum_{p=0}^{N} \sum_{i=0}^{N} \Theta_{pi} X_i \sum_{j=0}^{N} \frac{M_{jp}^{-1}}{B_{n_j,j}((M^{-1}X)_j)} \frac{\partial B_{n_j,j}}{\partial x}((M^{-1}X)_j) = \sum_{j=0}^{N} \Lambda_{jj}(M^{-1}X)_j \frac{1}{B_{n_j,j}((M^{-1}X)_j)} \frac{\partial B_{n_j,j}}{\partial x}((M^{-1}X)_j)$$

$$= \sum_{j=0}^{N} \frac{\Lambda_{jj}}{d_j}(-\frac{1}{B_{n_j,j}((M^{-1}X)_j)} \frac{\partial^2 B_{n_j,j}}{\partial x^2}((M^{-1}X)_j) - \lambda_{n_j,j})$$

Taking a look at the next term, using the fact that M is orthogonal and that thus $M^{-1} = M^T$, and that $\gamma_p = 1$, we see:

$$\sum_{p=0}^{N} \frac{1}{\gamma_p}(M_{jp}^{-1})^2 = \sum_{p=0}^{N} M_{jp}^{-1} M_{pj} = (M^{-1}M)_{jj} = 1$$

We conclude

$$\sum_{p=0}^{N} \frac{1}{\gamma_p} \sum_{j=0}^{N} \frac{(M_{jp}^{-1})^2}{B_{n_j,j}((M^{-1}X)_j)} \frac{\partial^2 B_{n_j,j}}{\partial x^2}((M^{-1}X)_j) = \sum_{j=0}^{N} \frac{1}{B_{n_j,j}((M^{-1}X)_j)} \frac{\partial^2 B_{n_j,j}}{\partial x^2}((M^{-1}X)_j)$$

For the consequent, we note that for $l \neg j$, we have

$$\sum_{p=0}^{N} M_{jp}^{-1} M_{lp}^{-1} = \sum_{p=0} M_{jp}^{-1} M_{pl} = (M^{-1}M)_{jl} = I_{jl} = 0$$

The term involving the sum over $l \neq j$ therefore completely drops out of the equation. The final equation thus gives:

$$\sum_{j=0}^{N} \frac{1 - \frac{\Lambda_{jj}}{d_j}}{B_{n_j,j}((M^{-1}X)_j)} \frac{\partial^2 B_{n_j,j}}{\partial x^2}((M^{-1}X)_j) + \lambda - \sum_{j=0}^{N} \frac{\Lambda_{jj}}{d_j} \lambda_{n_j,j} + \sum_{p=0}^{N} \Theta_{jj} = 0$$

Appendix D

Simulation Script

The following script was used to simulate the Langevin equation

```matlab
function [Var,t]=sim(vars);
N=10;
nu=0.588;
alpha=1+2*nu;
gammabar=1;

Lbar=vars(1);
Gamma_Pbar=vars(2);
k_1bar=vars(3);
s_1bar=vars(4);

Xi_amp=[2/gammabar;2/Gamma_Pbar*ones(N,1)];
K_pbar=k_1bar*(1:N).^(-alpha);
S_pbar=s_1bar*(1:N).^(-alpha);
Theta=diag([1 K_pbar]);
Theta(1,2:end)=S_pbar;
Theta(2:end,1)=S_pbar/Gamma_Pbar;

Xbelow0=[1;
zeros(N,1)];gammas=[gammabar ones(1,N)*Gamma_Pbar];

%integration parameters
t_0=0;
Y_0=Xbelow0;
t_end=1;
nt=1000;
realizations=500;

dt=(t_end-t_0)/(nt-1);
Y=zeros(N+1,nt);
Y(:,1)=Y_0;
X=zeros(nt,realizations,N+1);
Ncell=zeros(realizations,nt);
ncell=zeros(1,nt);
t=linspace(t_0,t_end,nt);

%integration
for n=1:realizations;
for i=2:nt;
Y(:,i)=Y(:,i-1)+(-Theta*Y(:,i-1)*dt+sqrt(dt)*Xi_amp.*randn(N+1,1));
```

```matlab
41   if Y(1,i)>=Lbar;
42   Y(1,i)=Y(1,i)-2*Lbar;
43   Ncell(n,i)=Ncell(n,i-1)+1;
44   Y(2:end,i)=0;
45   elseif Y(1,i)<=-Lbar;
46   Y(1,i)=Y(1,i)+2*Lbar;
47   Ncell(n,i)=Ncell(n,i-1)-1;
48   Y(2:end,i)=0;
49   else;
50   Ncell(n,i)=Ncell(n,i-1);
51   end
52   X(:,n,:)=Y(:,:)'+[2*Lbar*Ncell(n,:);zeros(N,nt)]';
53   end
54   end
55   Mean=mean(X(:,:,1)');
56   Var=var(X(:,:,1)');
```

Appendix E

Application of changing boundary conditions

This script was used when obtaining an exact solution to the Fokker-Planck equation.

```matlab
clear all
vars=[1 1 1 0.1];

N=1;
nu=0.588;
alpha=1+2*nu;
gammabar=1;

Lbar=vars(1);
Gamma_Pbar=vars(2);
k_1bar=vars(3);
s_1bar=vars(4);

Xi_amp=[2/gammabar;2/Gamma_Pbar*ones(N,1)];
K_pbar=k_1bar*(1:N).^(-alpha);
S_pbar=s_1bar*(1:N).^(-alpha);
Theta=diag([1 K_pbar]);
Theta(1,2:end)=S_pbar;
Theta(2:end,1)=S_pbar/Gamma_Pbar;
[M,Lambda]=eig(Theta);
Mmin=inv(M);

Xbelow0=zeros(N+1,1);%initial position
gammas=[gammabar ones(1,N)*Gamma_Pbar];

%%
%p0=@(X) dirac(X(1,:)).*dirac(X(2,:));
a=@(X) X(1,:).*exp(-Theta(2,2)*X(2,:).^2);
b=@(X) exp(-Theta(2,2)*X(2,:).^2);
%%
neig=3;
x=linspace(-Lbar,Lbar);

%%Eigenfunctions
Bnotnormed= @(x,n,j) exp(-Lambda(j,j)*x.^2/2).*hermiteH(n,x*(sqrt(Lambda(j,j)/2)));

```

```matlab
37  integrals=zeros(neig,length(Lambda));
38  for n=1:neig;
39  for j=1:length(Lambda);
40  f= @(x) Bnotnormed(x,n,j).^2;
41  integrals(n,j)=integral(f,-Inf,Inf);
42  end
43  end
44
45  Bb= @(x,n,j)  integrals(n,j).^(-1/2).*exp(-Lambda(j,j)*x.^2/2).*hermiteH(n,x
        *(sqrt(Lambda(j,j)/2)));
46  ns=allcomb(1:neig,1:neig);
47  lambdab=@(n,j)Lambda(j,j)*(n+1);
48  Bn=@(X,n)  Bb(Mmin(1,:)*X,ns(n,1),1).*Bb(Mmin(2,:)*X,ns(n,2),2);
49  lambda=@(n)  lambdab(ns(n,1),1)+lambdab(ns(n,2),2)-sum(diag(Theta));
50  h=1e-4;
51
52  %%
53  intx=linspace(-5,5);
54  Labn=@(X,n)  (trace(Theta)*a(X)+diag([[(a(X+repmat([h;0],1,iscolumn(X)+(1-
        iscolumn(X))*length(X)))-a(X))/h; (a(X+repmat([0;h],1,iscolumn(X)+(1-
        iscolumn(X))*length(X)))-a(X))/h]'*Theta*X)'+(a(X+repmat([h;0],1,
        iscolumn(X)+(1-iscolumn(X))*length(X)))-2*a(X)+a(X+repmat([-h;0],1,
        iscolumn(X)+(1-iscolumn(X))*length(X))))/(h^2)+ (a(X+repmat([0;h],1,
        iscolumn(X)+(1-iscolumn(X))*length(X)))-2*a(X)+a(X+repmat([0;-h],1,
        iscolumn(X)+(1-iscolumn(X))*length(X))))/(h^2)).*Bn(X,n);
55  abn=@(X,n)  a(X).*Bn(X,n);
56  Lbbn=@(X,n)  (trace(Theta)*b(X)+diag([[(b(X+repmat([h;0],1,iscolumn(X)+(1-
        iscolumn(X))*length(X)))-b(X))/h; (b(X+repmat([0;h],1,iscolumn(X)+(1-
        iscolumn(X))*length(X)))-b(X))/h]'*Theta*X)'+(b(X+repmat([h;0],1,
        iscolumn(X)+(1-iscolumn(X))*length(X)))-2*b(X)+b(X+repmat([-h;0],1,
        iscolumn(X)+(1-iscolumn(X))*length(X))))/(h^2)+ (b(X+repmat([0;h],1,
        iscolumn(X)+(1-iscolumn(X))*length(X)))-2*b(X)+b(X+repmat([0;-h],1,
        iscolumn(X)+(1-iscolumn(X))*length(X))))/(h^2)).*Bn(X,n);
57  bbn=@(X,n)  b(X).*Bn(X,n);
58  p0bn=@(X,n)  p0(X).*Bn(X,n);
59  h=waitbar(0,'double integrals');
60  for n=1:length(ns);
61  waitbar(n/length(ns),h,'double integrals');
62  for index=1:length(x);
63  Labnn=@(y)  Labn([x(index)*ones(1,length(y));y],n);
64  Labints(n,index)=mean(Labnn(intx))*10;
65  abnn=@(y)  abn([x(index)*ones(1,length(y));y],n);
66  abints(n,index)=mean(abnn(intx))*10;
67  Lbbnn=@(y)  Lbbn([x(index)*ones(1,length(y));y],n);
68  Lbbints(n,index)=mean(Lbbnn(intx))*10;
69  bbnn=@(y)  bbn([x(index)*ones(1,length(y));y],n);
70  bbints(n,index)=mean(bbnn(intx))*10;
71  Bnbnn=@(y)  Bn([x(index)*ones(1,length(y));y],n).^2;
72  Bnbints(n,index)=mean(Bnbnn(intx))*10;
73  %p0bnn=@(y)  p0bn([x(index)*ones(1,length(y));y],n);
74  %p0bints(n,index)=integral(p0bnn,-Inf,Inf);
75  end;
76  end;
77  close(h);
78  Labint=2*Lbar*mean(Labints');
79  abint=2*Lbar*mean(abints');
```

```matlab
80  Lbbint=2*Lbar*mean(Lbbints');
81  bbint=2*Lbar*mean(bbints');
82  Bnbint=2*Lbar*mean(Bnbints');
83  %p0bint=2*Lbar*mean(p0bints');
84  %%
85  Bint=zeros(length(ns),length(x));
86  aint=zeros(1,length(x));
87  bint=zeros(1,length(x));
88  for index=1:length(x);
89  an=@(y) a([x(index)*ones(1,length(y));y]);
90  bn=@(y) b([x(index)*ones(1,length(y));y]);
91  aint(index)=integral(an,-Inf,Inf);
92  bint(index)=integral(bn,-Inf,Inf);
93
94  for n=1:length(ns);
95  Bnn=@(y) Bn([x(index)*ones(1,length(y));y],n);
96  Bint(n,index)=integral(Bnn,-Inf,Inf);
97  end;
98  end;
99  %%
100 [topleftnum,topleftden]=largepolsum(lambda(1:length(ns))',-abint.*Bint(1:
        length(ns),end)'./Bnbint,Bint(1:length(ns),end)'.*Labint./Bnbint);
101 topleftnum=topleftnum+aint(end)*poly(-lambda(1:length(ns)));
102 [toprightnum,toprightden]=largepolsum(lambda(1:length(ns))',-bbint.*Bint(1:
        length(ns),end)'./Bnbint,Bint(1:length(ns),end)'.*Lbbint./Bnbint);
103 topleftnum=topleftnum+bint(end)*poly(-lambda(1:length(ns)));
104 [botleftnum,botleftden]=largepolsum(lambda(1:length(ns))',-abint.*Bint(1:
        length(ns),1)'./Bnbint,Bint(1:length(ns),1)'.*Labint./Bnbint);
105 botleftnum=botleftnum+aint(1)*poly(-lambda(1:length(ns)));
106 [botrightnum,botrightden]=largepolsum(lambda(1:length(ns))',-bbint.*Bint(1:
        length(ns),1)'./Bnbint,Bint(1:length(ns),end)'.*Lbbint./Bnbint);
107 botrightnum=botrightnum+bint(1)*poly(-lambda(1:length(ns)));
108
109 [topnum,topden]=largepolsum(lambda(1:length(ns))',zeros(1,length(ns)),Bint
        (1:length(ns),end)'.*p0bint./Bnbint);
110 [botnum,botden]=largepolsum(lambda(1:length(ns))',zeros(1,length(ns)),Bint
        (1:length(ns),1)'.*p0bint./Bnbint);
111 %%
112 Anum=conv(botrightnum,topnum)-conv(toprightnum,botnum);
113 Aden=conv(botrightnum,topleftnum)-conv(toprightnum,botleftnum);
114
115 Bnum=-conv(botleftnum,topnum)+conv(topleftnum,botnum);
116 Bden=conv(botrightnum,topleftnum)-conv(toprightnum,botleftnum);
117
118 %%
119 at=pol2func(Anum,Aden);
120 bt=pol2func(Bnum,Bden);
121 marginalprobability=@(t) aint*at(t)+bint*bt(t);
122 for n=1:length(ns);
123 n
124 ant=pol2func(conv(Anum,[-abint(n) Labint(n)]),conv(Aden,[1 lambda(n)]));
125 n+100
126 bnt=pol2func(conv(Bnum,[-bbint(n) Lbbint(n)]),conv(Bden,[1 lambda(n)]));
127 marginalprobability=@(t) marginalprobability(t)+(ant(t)+bnt(t)+p0bint(n)*
        exp(-lambda(n)*t))*Bint(n,:)/Bnbint(n);
128 end
```

Two functions are called upon in the process, these are included below.

```matlab
function [f] = pol2func(numerator,denominator)
[r,p,k]=residue3(numerator,denominator);
f=@(t) sum(r.*exp(t*p));
```

```matlab
function [coeffs,poles,k] = residue3(u,v)
poles=roots(v)';
u=u/v(1);
matrix=zeros(length(v));
matrix(:,1)=v';
for j=1:length(poles);
matrix(2:end,j+1)=poly([poles(1:j-1) poles(j+1:end)])';
end
matrix=matrix./repmat(u'+(u'==0),1,length(v));
sol=matrix\(ones(length(v),1)-(u'==0));
coeffs=sol(2:end)';
k=sol(1);
```

Bibliography

[1] M. Abramowitz and I. A. Stegun. *Handbook of Mathematical Functions with Formulas Graphs and Formulas.* United States Department of Commerce, National Bureau of Standards, 1964.

[2] I.Y.Wong, M. L. Gardel, D. R. Reichman, Eric R.Weeks, M.T. Valentine, A. R. Bausch, and D. A.Weitz. *Physical review letters.*

[3] K. Luo, S. T. T. Ollila, I. Huopaniemi, T Ala-Nissila, P. Pomorski, M. Karttunen, S. Ying, , and A. Bhattacharya. Dynamical scaling exponents for polymer translocation through a nanopore. *Physical review. E, Statistical, nonlinear, and soft matter physics*, 2008.

[4] L. Masaro and X.X. Zhu. Physical models of diffusion for polymer solutions, gels and solids. *Progress in polymer science*, 1999.

[5] J. T. Padding. *Theory of Polymer Dynamics.* University of Cambridge, 2006.

[6] T. Pakula. Cooperative relaxations in condensed macromolecular systems. 1. a model for computer simulation. *Macromolecules*, 1987.

[7] H. Risken. *The Fokker-Planck Equation.* Springer-Verlag, 1984.

[8] S. Walta, F. Di Lorenzo, K. Ma, U. Wiesner, and W. Richtering. Diffusion of rigid nanoparticles in crowded polymer-network hydrogels: dominance of segmental density over crosslinking density. *Colloid and Polymer Science*, 2017.